High-Pressure NMR and *ab Initio* Computational Studies on the Insertion Mechanism of Carbon Monoxide into Cationic Monoorganopalladium(II) Complexes Bearing Tridentate Nitrogen Donor Ligands

Bertus A. Markies,[†] Peter Wijkens,[†] Alain Dedieu,*[,§,||] Jaap Boersma,*[,†]
Anthony L. Spek,[‡,⊥] and Gerard van Koten[†]

*Debye Institute, Department of Metal-Mediated Synthesis, Utrecht University,
Padualaan 8, 3584 CH Utrecht, The Netherlands, Bijvoet Center for Biomolecular Research,
Laboratory of Crystal and Structural Chemistry, Utrecht University,
Padualaan 8, 3584 CH Utrecht, The Netherlands, and Laboratoire de Chimie
Quantique, UPR 139 du CNRS, Université Louis Pasteur, 4 Rue Blaise Pascal,
67070 Strasbourg Cédex, France*

A number of methyl and arylpalladium(II) cations bearing tridentate nitrogen-donor ligands has been prepared, and their reactivity in the insertion of carbon monoxide has been studied. The resulting acetyl and aroylpalladium complexes of the ligands *N*-(2-picolyl)-*N*,*N'*,*N'*-trimethylethylenediamine (pico) and *N*,*N*,*N'*,*N''*,*N''*-pentamethyldiethylenetriamine (pmdeta) were isolated and characterized. In the case of the 4-nitrophenylpalladium and 2,4,6-trimethylphenylpalladium pico- and pmdeta complexes, no carbonylation products could be isolated. In these cases, either the equilibrium of the carbonylation reaction did not lie fully to the side of the insertion product even at 10 atm of CO or the insertion product decarbonylated upon attempted isolation. The methylpalladium complex of the 2,6-bis-[(dimethylamino)methyl]pyridine (NN'N) ligand reacted quantitatively with CO in CD$_3$-COCD$_3$ to give acetic anhydride, palladium metal, and the protonated ligand; a mechanism for the anhydride formation is proposed. With the exception of the 1-naphthoyl derivative, the aroyl complexes of the NN'N ligand could not be isolated due to decarbonylation upon attempted isolation. Most of the unstable insertion products could, however, be characterized by IR and high-pressure NMR. Crystals of the 1-naphthoylpalladium complex with the NN'N ligand were obtained from acetone/pentane under a CO atmosphere. This complex is the first example of an aroylpalladium(II) cation. Two reaction pathways for the carbonyl insertion reaction, *i.e.*, dissociative and associative, have been evaluated using ^{1}H NMR studies and *ab initio* calculations. The insertion reaction at 10 atm of CO pressure in CD$_3$-COCD$_3$ is complete within 2.5 min for most complexes, with the exception of those bearing strongly electron-withdrawing para substituents (*e.g.*, NO$_2$) or sterically demanding ortho substituents (*e.g.*, 2,4,6-trimethyl) on the aryl ring. *Ab initio* calculations at the RHF, MP2//SCF, and CAS−SCF/CI levels on the cationic model system [Pd(CH$_3$)(NH$_3$)$_3$]$^+$ + CO and the neutral system [Pd(CH$_3$)$_2$(NH$_3$)$_2$] + CO show that the carbonylation reaction follows a hybrid pathway, *i.e.*, a concerted replacement of NH$_3$ by CO followed by migratory insertion of CO into the Pd−C bond instead of a purely dissociative or associative mechanism. For both the neutral and the cationic systems the rate-determining step is the migratory insertion. The insertion process is enhanced by coordination of the dissociated amine and is slightly more favorable in the neutral system. Together with the low-energy replacement of NH$_3$ by CO, this implies that in both systems the rate of carbonyl insertion should be independent of the applied CO pressure.

Introduction

The insertion of carbon monoxide into metal-to-carbon σ-bonds is one of the most important steps in homogeneous catalysis by transition metal complexes.[1] It is generally accepted, both on experimental[1,2] and theoretical[3] grounds, that CO insertion involves migration of the hydrocarbyl group to the coordinated CO ligand. Very recently, Van Leeuwen *et al.* presented evidence for such migration in the case of square planar palladium and platinum bidentate diphosphine complexes.[4] Garrou and Heck showed that, in *trans*-MXR(PR$_3$)$_2$

---

(1) (a) Parshall, G. W.; Ittel, S. D. *Homogeneous Catalysis. The Applications and Chemistry of Catalysis by Soluble Transition Metal Complexes*, 2nd ed.; Wiley: New York, 1992. (b) Collman, J. P.; Hegedus, L. S.; Norton, J. R.; Finke, R. G. *Principles and Applications of Organotransition Metal Chemistry*; Oxford University Press: Oxford, 1987.
(2) Ozawa, F.; Yamamoto, A. *Chem. Lett.* **1981**, 289.

complexes (M = Pd or Pt; R = alkyl or aryl; X = I, Br, Cl), insertion proceeds via an initial five-coordinate intermediate MXR(CO)(PR$_3$)$_2$ and then follows a dissociative or a migratory pathway.[5] In the dissociative pathway, which is slowed down in the presence of excess phosphine, this intermediate loses one phosphine ligand prior to CO insertion, which then proceeds from a four-coordinate complex. In the migratory pathway direct CO insertion occurs.

Little is known about the insertion mechanism when bi-[6] or tridentate donor ligands[6j,7,8] are used. Early studies by Anderson and Lumetta suggested the dissociation of one of the chelate donor atoms when mixed phosphorus/sulfur (P–S) or phosphorus/nitrogen (P–N) ligands were used.[6f] Cavell *et al.* observed similar effects in the carbonylation of palladium(II) complexes PdMe(XY)(PPh$_3$) in which XY is a β-diketonate or a monothio-β-diketonate ligand.[6n,o] Van Leeuwen and Vrieze *et al.*[6d,g] recently investigated the influence of the bite angle of the ligand for both neutral and cationic complexes of the type PdClMe(P–P) on the insertion rate.

So far, only two reports have appeared on the carbonylation of palladium(II) complexes containing a terdentate ligand, both of which describe complexes of
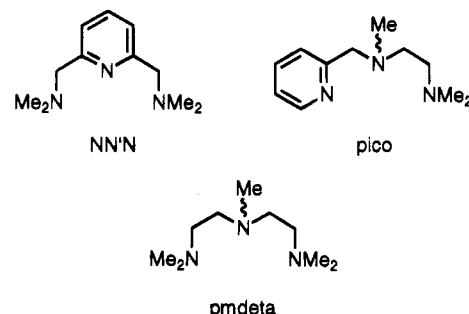
(3) For semiempirical calculations see: (a) Berke, H.; Hoffmann, R. *J. Am. Chem. Soc.* **1978**, *100*, 7224. (b) Ruiz, M. E.; Flores-Riveros, A.; Novaro, O. *J. Catal.* **1980**, *64*, 1. (c) Calhorda, M. J.; Brown, J. M.; Cooley, N. A. *Organometallics* **1991**, *10*, 1431. For ab initio calculations see: (d) Sakaki, S.; Kitaura, K.; Morokuma, K.; Ohkubo, K. *J. Am. Chem. Soc.* **1983**, *105*, 2280. (e) Koga, N.; Morokuma, K. *J. Am. Chem. Soc.* **1986**, *108*, 6136. (f) Ziegler, T.; Versluis, L.; Tschinke, V. *J. Am. Chem. Soc.* **1986**, *108*, 612. (g) Axe, F. U.; Marynick, D. S. *Organometallics* **1987**, *6*, 572. (h) Dedieu, A.; Sakaki, S.; Strich, A.; Siegbahn, P. E. M. *Chem. Phys. Lett.* **1987**, *133*, 317. (i) Shusterman, A. J.; Tamir, I.; Pross, A. *J. Organomet. Chem.* **1988**, *340*, 203. (j) Versluis, L.; Ziegler, T.; Baerends, E. J.; Ravenek, W. *J. Am. Chem. Soc.* **1989**, *111*, 2018. (h) Koga, N.; Morokuma, K. *New J. Chem.* **1991**, *15*, 749. (k) Koga, N.; Morokuma, K. *Chem. Rev.* **1991**, *91*, 823. (l) Tchougreeff, A. L.; Gulevich, Yu. V.; Misurkin, I. A.; Beletskaya, I. P. *J. Organomet. Chem.* **1993**, *455*, 261. (m) Blomberg, M. R. A.; Karlsson, C. A. M.; Siegbahn, P. E. M. *J. Phys. Chem.* **1993**, *97*, 9341.

(4) Van Leeuwen, P. W. N. M.; Roobeek, C. F.; Van der Heijden, H. *J. Am. Chem. Soc.* **1994**, *116*, 12117.

(5) Garrou, P. E.; Heck, R. F. *J. Am. Chem. Soc.* **1976**, *98*, 4115.

(6) For P–P complexes see: (a) Bennett, M. A.; Rokicki, A. *J. Organomet. Chem.* **1983**, *244*, C31. (b) Ozawa, F.; Hayashi, T.; Koide, H.; Yamamoto, A. *J. Chem. Soc., Chem. Commun.* **1991**, 1469. (c) Dekker, G. P. C. M.; Elsevier, C. J.; Vrieze, K.; van Leeuwen, P. W. N. M.; Roobeek, C. F. *J. Organomet. Chem.* **1992**, *430*, 357. (d) Dekker, G. P. C. M.; Elsevier, C. J.; Vrieze, K.; van Leeuwen, P. W. N. M. *Organometallics* **1992**, *11*, 1598. (e) Tóth, I.; Elsevier, C. J. *J. Chem. Soc., Chem. Commun.* **1993**, 529. For P–N complexes see: (f) Anderson, G. K.; Lumetta, G. J. *Organometallics* **1985**, *4*, 1542. (g) Dekker, G. P. C. M.; Buijs, A.; Elsevier, C. J.; Vrieze, K.; van Leeuwen, P. W. N. M.; Smeets, W. J. J.; Spek, A. L.; Wang, Y. F.; Stam, C. H. *Organometallics* **1992**, *11*, 1937. For N–N complexes see: (h) de Graaf, W.; Boersma, J. van Koten, G. *Organometallics* **1990**, *9*, 1479. (i) Markies, B. A.; Rietveld, M. H. P.; Boersma, J.; Spek, A. L.; van Koten, G. *J. Organomet. Chem.* **1992**, *424*, C12. (j) Rülke, R. E. Thesis, University of Amsterdam, Amsterdam, The Netherlands, 1995. (k) Brookhart, M.; Rix, F. C.; DeSimone, J. M. *J. Am. Chem. Soc.* **1992**, *114*, 5894. (l) van Asselt, R.; Gielens, E. E. C. G.; Rülke, R. E.; Elsevier, C. J. *J. Chem. Soc., Chem. Commun.* **1993**, 1203. (m) Markies, B. A.; Verkerk, K. A. N.; Rietveld, M. H. P.; Boersma, J.; Kooijman, H.; Spek, A. L.; van Koten, G. *ibid.* **1993**, 1317. Other ligands or mixed systems: (n) Anderson, G. K.; Lumetta, G. J. *Organometallics* **1985**, *4*, 1542. (o) Cavell, K. J.; Jin, H.; Skelton, B. W.; White, A. H. *J. Chem. Soc., Dalton Trans.* **1992**, 2923. (p) Cavell, K. J.; Jin, H.; Skelton, B. W.; White, A. H. *ibid.* **1993**, 1973. (q) Lindner, E.; Dettinger, J.; Fawzi, R.; Steimann, M. *Chem. Ber.* **1993**, *126*, 1347. (r) Reger, D. L.; Garza, D. G. *Organometallics* **1993**, *12*, 554.

(7) (a) Rülke, R. E.; Han, I. M.; Elsevier, C. J.; Vrieze, K.; van Leeuwen, P. W. N. M.; Roobeek, C. F.; Zoutberg, M. C.; Wang, Y. F.; Stam, C. H. *Inorg. Chim. Acta* **1990**, *169*, 5. (b) Wehman, P.; Rülke, R. E.; Kaasjager, V. E.; Kamer, P. C. J.; Koopman, H.; Spek, A. L.; Elsevier, C. J.; Vrieze, K.; van Leeuwen, P. W. N. M. *J. Chem. Soc., Chem. Commun.* **1995**, 331.

(8) Markies, B. A.; Wijkens, P.; Boersma, J.; Spek, A. L.; van Koten, G. *Recl. Trav. Chim. Pays-Bas* **1991**, *110*, 133.

Table 1. Summary and Numbering of the Complexes

	R–Pd			R–CO–Pd		
R	NN'N	pico	pmdeta	NN'N	pico	pmdeta
Me	**1a**	**2a**	**3a**		**5a**	**6a**
Ph	**1b**	**2b**	**3b**	**4b**	**5b**	**6b**
4-O$_2$NC$_6$H$_4$	**1c**	**2c**	**3c**	**4c**	**5c**	**6c**
2-MeC$_6$H$_4$	**1d**	**2d**	**3d**	**4d**	**5d**	**6d**
1-naphthyl	**1e**	**2e**	**3e**	**4e**	**5e**	**6e**
mesityl[a]	**1f**	**2f**	**3f**	**4f**	**5f**	**6f**

[a] 2,4,6-Trimethylphen-1-yl.

N-donor ligands. Vrieze *et al.* reported the synthesis and subsequent carbonylation of the methylpalladium-(II) complexes [PdMe(terpy)]Cl·2H$_2$O, PdClMe(*i*-Pr-DIP), and [PdMe(*i*-Pr-DIP)]OTf (terpy = 2,2':6',2''-terpyridyl; *i*-Pr-DIP = 2,6-bis(N-isopropylcarbaldimino)pyridine),[7] and we gave a preliminary account of the synthesis and carbonylation of arylpalladium(II) complexes of the type [PdAr(NN'N)]OTf with Ar = phenyl or 1-naphthyl and NN'N = 2,6-bis[(dimethylamino)-methyl]pyridine.[8] We chose tridentate ligands to diminish the degrees of freedom for rearrangements around the metal center.

In the present paper we present the results of high-pressure NMR measurements and *ab initio* calculations on the carbonyl insertion reaction of palladium complexes containing the NN'N, pmdeta (N,N,N',N'',N''-pentamethyldiethylenetriamine), and pico (N,N,N'-trimethyl-N'-(2-picolyl)ethylenediamine) ligands.

NN'N   pico
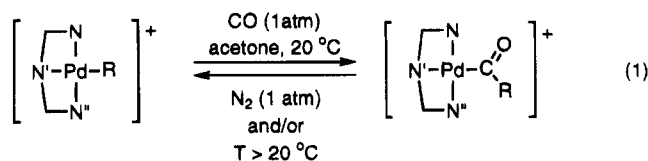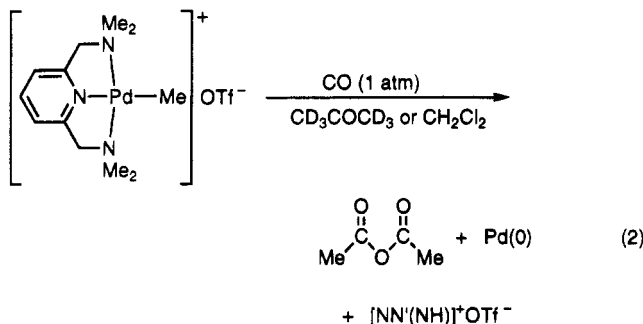

pmdeta

Results

Insertion and Deinsertion of Carbon Monoxide. The methyl (**1–3a**) and aryl compounds (**1b–f**, **2b–e**, and **3b–f**) used in this study were prepared via reported procedures and are listed in Table 1.[9]

Insertion of carbon monoxide (eq 1) was performed

$$(1)$$

by bubbling CO at atmospheric pressure through a CD$_3$-

(9) Markies, B. A.; Wijkens, P.; Kooijman, H.; Veldman, N.; Spek, A. L.; Boersma, J.; van Koten, G. *Organometallics* **1994**, *13*, 3244.

COCD$_3$ solution of the methyl and aryl complexes at room temperature. Decarbonylation of the CO-insertion products was carried out by bubbling nitrogen gas through the solution and/or heating the solution (up to 55 °C, *i.e.*, the boiling point of CD$_3$COCD$_3$).

The NN'N-coordinated methyl complex (**1a**) reacted at atmospheric pressure with CO in CD$_3$COCD$_3$ to give palladium metal, the quaternary ammonium salt [NN'-(NH)]OTf, and acetic anhydride in 84% yield (calculated on **1a**) (eq 2). Acetic anhydride was also obtained when

$$\left[\begin{array}{c}\text{Me}_2\\ \text{N}\\ \\ \text{N—Pd—Me}\\ \\ \text{N}\\ \text{Me}_2\end{array}\right]^+ \text{OTf}^- \xrightarrow[\text{CD}_3\text{COCD}_3 \text{ or } \text{CH}_2\text{Cl}_2]{\text{CO (1 atm)}}$$

$$\underset{\text{Me}}{\overset{\text{O}}{\underset{\|}{\text{C}}}}\underset{\text{O}}{\overset{\text{O}}{\underset{\|}{\text{C}}}}\underset{\text{Me}}{\text{}} + \text{Pd(0)} \qquad (2)$$

$$+ \text{[NN'(NH)]}^+\text{OTf}^-$$

this reaction was carried out in methylene chloride that had been predried over calcium hydride. Apparently, the acetyl complex is extremely easily hydrolyzed by traces of water. In contrast, the pico- and pmdeta-coordinated methyl complexes (**2a** and **3a**, respectively) gave the corresponding acetyl complexes (**5** and **6a**) as isolable solids, which were readily crystallized from methanol/diethyl ether without apparent methanolysis.

Most of the aryl complexes insert carbon monoxide at 1 atm to give the corresponding aroyl complexes (eq 1). Exceptions are the complexes containing 4-nitrophenyl (**1c**, **2d**, and **3d**) or 2,4,6-trimethylphenyl (mesityl, **1f**, **2e**, and **3e**) groups, which show only partial insertion at 1 atm, and the insertion products could not be isolated in pure form. The insertion equilibrium (eq 1) was shifted to the right by applying higher pressures (10−25 atm of CO) in a high-pressure NMR tube. In this way, ^{1}H and ^{13}C NMR spectra of the unstable products were obtained *in situ*, except for **4c,f**, which decomposed significantly during the ^{13}C NMR experiments, allowing only ^{1}H NMR spectra to be obtained. The benzoyl (**5b** and **6b**), and 4-methoxybenzoyl (**5c** and **6c**) complexes were purified by recrystallization from methanol/diethyl ether without apparent methanolysis. The 1-naphthoyl complex **4e** was successfully recrystallized from acetone/pentane under a CO atmosphere, and its solid state structure has been determined.

High-Pressure NMR Studies on the Insertion of Carbon Monoxide. We studied the insertion of carbon monoxide in CD$_3$COCD$_3$ solution at 10 atm of CO using a 10 mm high-pressure NMR tube[10] at 295 K. Under these conditions most of the complexes reacted completely to the corresponding acyl complexes within 2.5 min (the minimum time for the first spectrum to be obtained). The 4-nitrophenyl (**1c**, **2d**, and **3d**) and mesityl (**1f** and **2e**) complexes reacted much more slowly, but a reasonable to good conversion (79%−100%) was reached within 60 min. The mesityl complex **3e** did not react at all under these conditions (Table 2).

The methyl complex **1a** reacted within 2.5 min to give the same hydrolysis products as obtained at atmo-

(10) Roe, D. C. *J. Magn. Reson.* **1985**, *63*, 388.

Table 2. Influence of the Aryl Group on CO Insertion Time

ligand	R	time (min)	conversion (%)^a
NN'N	4-O$_2$NC$_6$H$_4$ (**1c**)	20	89
	mesityl^b (**1f**)	45	100
pico	4-O$_2$NC$_6$H$_4$ (**2d**)	36	100
	mesityl^b (**2e**)	60	79
pmdta	4-O$_2$NC$_6$H$_4$ (**3d**)	60	34
	mesityl^b (**3e**)	60	0

^{a} Conversion at 10 atm of CO and 296 K. ^{b} 2,4,6-Trimethylphen-1-yl.
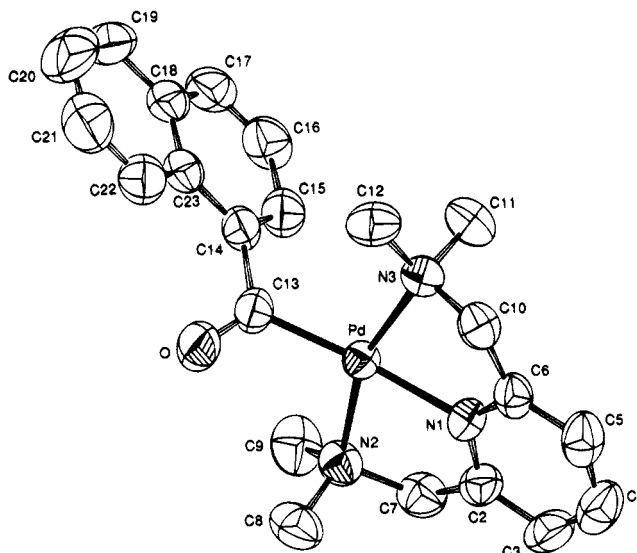
Figure 1. ORTEP representation (50% probability) of the cation [Pd(COC$_{10}$H$_7$)(NN'N)]$^+$ (**4e**).

Table 3. Selected Bond Distances (Å) and Angles (deg) of the Cation [Pd(1-naphthoyl)(NN'N)]$^+$ (4e)

Pd−N(1)	2.042(4)	Pd−C(13)	1.966(6)
Pd−N(2)	2.120(5)	C(13)−O	1.205(9)
Pd−N(3)	2.118(5)	C(13)−C(14)	1.509(10)
N(1)−Pd−N(2)	80.6(2)	N(3)−Pd−C(13)	100.7(2)
N(1)−Pd−N(3)	79.3(2)	Pd−C(13)−O	119.0(5)
N(1)−Pd−C(13)	172.4(3)	Pd−C(13)−C(14)	120.8(5)
N(2)−Pd−N(3)	159.7(2)	O−C(13)−C(14)	120.3(6)
N(2)−Pd−C(13)	99.6(2)		

spheric pressure. Attempts to follow the deinsertion of the carbonylation products (obtained at 10 atm of CO) by ^{1}H NMR, after release of the pressure, failed because this process was very slow. Apparently, for the deinsertion to proceed at a reasonable rate, nitrogen gas needs to be bubbled through the solution. Attempted deinsertion by raising the temperature to 55 °C (the boiling point of CD$_3$COCD$_3$) also failed, since decomposition to palladium metal is faster than deinsertion under these conditions.

Molecular Structure of the Cation [Pd(1-naphthoyl)(NN'N)]$^+$ (4e). The molecular structure of this cation is shown in Figure 1 with relevant bond distances and angles presented in Table 3. This structure is the first example of an aroylpalladium(II) cation.

In this square planar palladium(II) complex the 1-naphthoyl group is bonded *via* the carbonyl carbon atom in a position trans to the pyridine nitrogen atom N(1). The nitrogen atoms of the CH$_2$NMe$_2$ groups, N(2) and N(3), are bonded mutually trans, forming two fixed PdNCCN(1) five-membered chelate rings. These two chelate rings are puckered with an angle of 15.2(3)° between the mean planes through N1, N2, N3, and C13
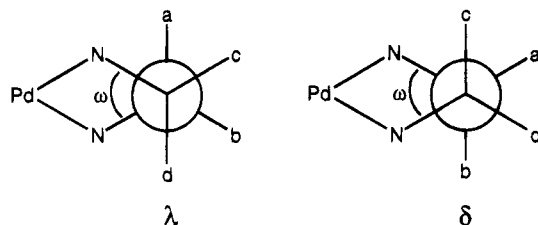
Figure 2. Newman projections of the λ and δ conformations of a five-membered diamine chelate ring.

and the pyridine moiety. The Pd–N(1) bond distance (2.042(4) Å) is short in comparison with the Pd–N(pyridyl) bond distance (2.131(4) Å) trans to the methyl group in [PdMe(2,2'-bipyridyl)(γ-picoline)]BF$_4$.[11] The short Pd–N(1) bond is accompanied by a small N(2)–Pd–N(3) angle (159.67(19)°). Similar features are present in the related complexes [PdMe(NN'N)]OTf,[9] [PdCl(pico)]Cl,[9] [PdX(2,2':6,2''-terpyridyl)]Cl·2H$_2$O (X = Cl[12a] or Me[7]), [Pd(OH)(2,2':6,2''-terpyridyl)]ClO$_4$·H$_2$O,[12b] and [PdCl{2,6-bis(2-imidazolin-2-yl)pyridine}]Cl.[12c] Apparently, the tridentate ligand in these complexes is unable to accommodate a perfect square planar geometry. The Pd–C bond distance in **4e** (1.966(6) Å) is close to other reported Pd–C(acyl) bond distances.[13,14] The carbonyl group of the 1-naphthoyl ligand has a normal Pd–C(13)–O angle (119.0(5)°) and must hence be η^1-bonded to palladium; this angle is much smaller for an η^2-bonded carbonyl group.[15]
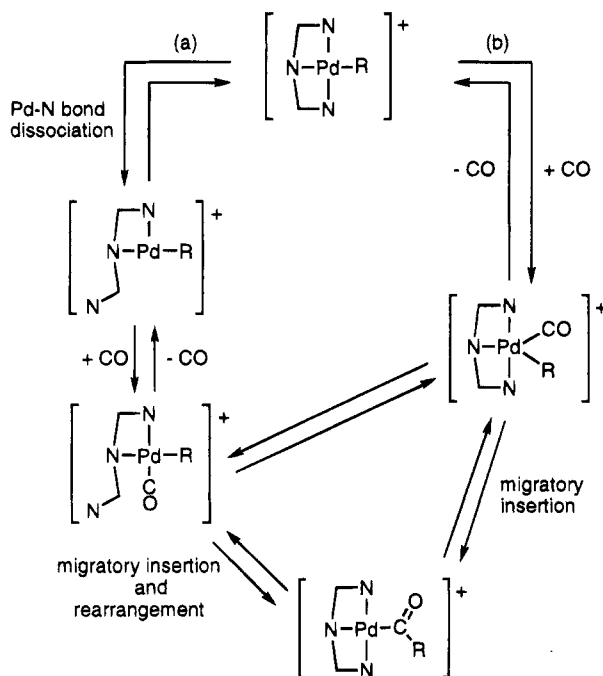
Solution Properties of the CO Insertion Products. The ^{1}H NMR resonances of the methylene protons of the pico ligand show well-defined multiplet (td) patterns at *ca.* 3.5 ppm and, in most cases, a poorly resolved ddd pattern at higher field. The patterns for these protons of the pmdeta ligand were much more complex, due to the small differences in chemical shift, but could still be analyzed by computer simulation. These patterns were used to determine the conformations of the NCH$_2$CH$_2$N chelate rings of the pico and pmdeta complexes as reported for the chloro, methyl, and aryl complexes of these ligands.[6b,c] The pico and pmdeta complexes all prefer the δ[17] or $\delta\delta$ conformation (Figure 2), respectively.

The $\delta\delta$ conformation of the pmdeta ligand is defined here with respect to the view of the complexes as depicted below.
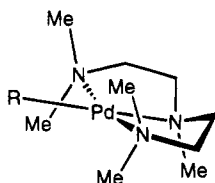
The analysis could not be carried out for [Pd(COMe)-(pmdeta)]OTf (**6a**) due to fluxionality of this complex (*vide infra*).

Scheme 1

The NMR spectra of the CO insertion products of the NN'N ligand (**4b–f**) showed in all cases well-defined resonances, with singlets for the CH$_2$ and NMe$_2$ groups, indicating that rotation around the Pd–C$_{CO}$ and C$_{CO}$–C$_{aryl}$ bonds is not hindered at ambient temperature (hindered rotation around the Pd–C$_{ipso}$ bond in arylpalladium NN'N complexes was found earlier[9]). The NMR spectra of the acetyl and aroyl pico (**5a–c**) and the aroyl pmdeta complexes (**6b,c**) also did not indicate hindered rotation, except for [Pd(COMe)(pmdeta)]OTf (**6a**). The resonances of the CH$_2$CH$_2$ moieties of **6a** are relatively broad at ambient temperature, become sharper on lowering the temperature to $\approx$271 K, and broaden again upon further lowering of the temperature.

***Ab Initio* Calculations of the Insertion Process.** To get some insight into the mechanism of the CO insertion process, we have carried out *ab initio* calculations on the cationic model system [Pd(CH$_3$)(NH$_3$)$_3$]$^+$ + CO. This model closely resembles the actual complexes and still allows reasonable geometry optimization calculations. Solvent effects were not incorporated at this stage, and thus the calculations should be viewed as providing information on the *intrinsic* ability of such cationic systems to follow a specific pathway. Our working hypothesis for the mechanism of the insertion reaction is outlined in Scheme 1.

(11) Byers, P. K.; Canty, A. J.; Skelton, B. W.; White, A. H. *J. Organomet. Chem.* **1987**, *336*, C55.

(12) (a) Intille, G. M.; Pfluger, C. E.; Baker, W. A., Jr. *J. Cryst. Mol. Struct.* **1973**, *3*, 47. (b) Castan, P.; Dahan, F.; Wimmer, S.; Wimmer, F. L. *J. Chem. Soc., Dalton Trans.* **1990**, 2679. (c) Baker, A. T.; Craig, D. C.; Singh, P. *Aust. J. Chem.* **1991**, *44*, 1659.

(13) (a) Fayos, J.; Dobrzynski, E.; Angelici, R. J.; Clardy, J. *J. Organomet. Chem.* **1973**, *59*, C33. (b) Bardi, R.; Piazessi, A. M.; Cavinato, G.; Cavoli, P.; Toniolo, L. *J. Organomet. Chem.* **1982**, *224*, 407. See also refs 3m and 4l.

(14) The structures of PdCl(COMe)(L$_2$), with L$_2$ = 2-(isopropylcarbaldimino)pyridine or 2,2'-bipyridyl, have been solved only recently and have Pd–C(acyl) bond distances of 1.964(5) and 1.94(1) Å, respectively. Rülke, R. E.; Elsevier, C. J.; Vrieze, K. Unpublished results.

(15) For a review on η^2-acyl coordination see: Durfee, L. D.; Rothwell, I. P. *Chem. Rev.* **1988**, *88*, 1059.

(16) (a) Sudmeier, J. L.; Blackmer, G. L. *Inorg. Chem.* **1971**, *10*, 2010. (b) Hawkins, C. J.; Peachey, R. M. *Aust. J. Chem.* **1976**, *29*, 33. (c) Hambley, T. W.; Hawkins, C. J.; Martin, J.; Palmer, J. A.; Snow, M. R. *Aust. J. Chem.* **1981**, *34*, 2505. (c) Hawkins, C. J.; Palmer, J. A. *Coord. Chem. Rev.* **1982**, *44*, 1.
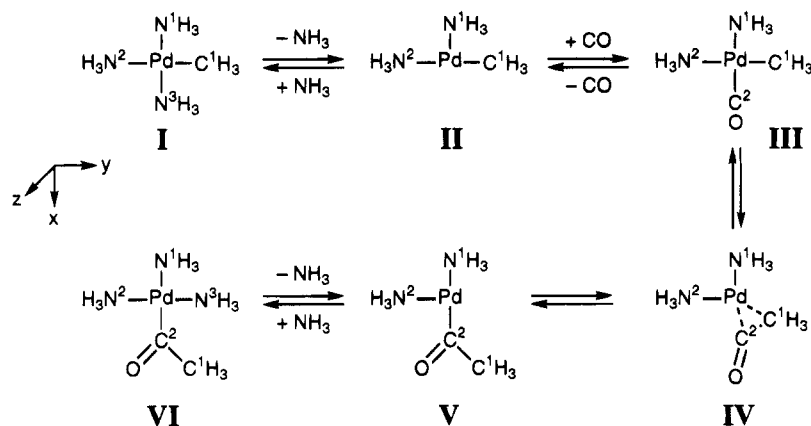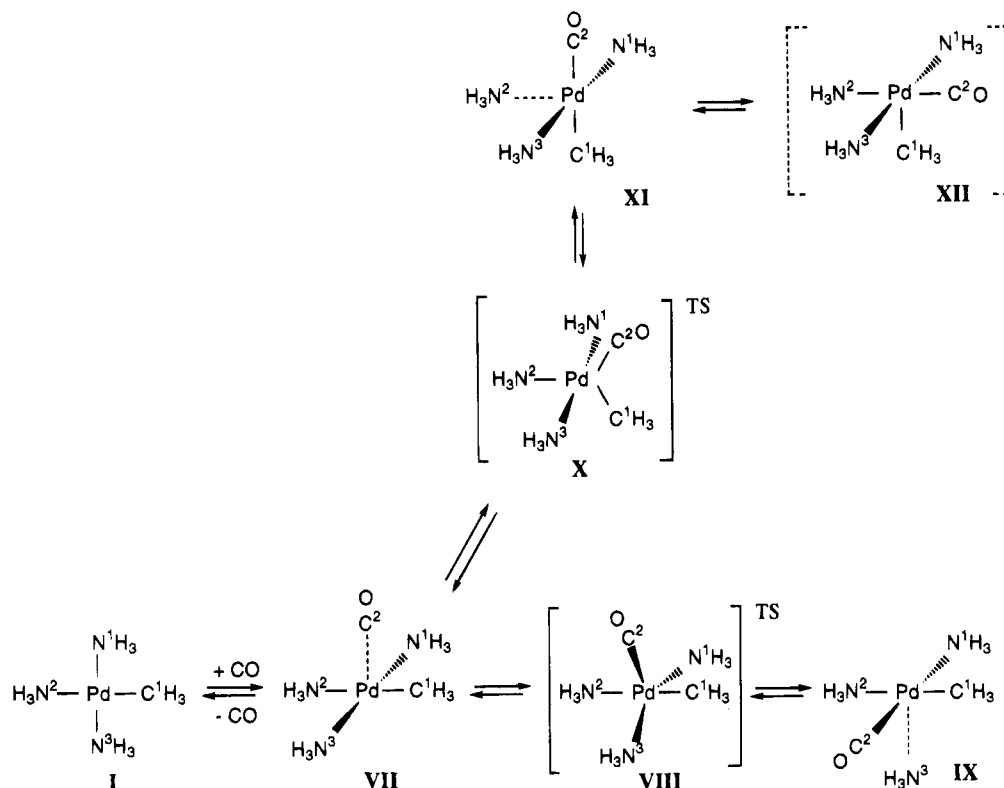
(17) The central NMe group of the pico complexes is chiral, and these complexes are obtained as a 1:1 mixture of enantiomers, with the enantiomer containing the *S* configuration showing the δ conformation. Because the two enantiomers have a reversed preference for the conformation of the NCCN chelate rings, the enantiomer with the *R* configuration for the NMe group will show the λ conformation.

Scheme 2

Scheme 3

Two main routes could be considered *a priori*: a purely dissociative one, a, in which one amine arm dissociates prior to CO coordination; and a purely associative one, b, in which CO coordinates first and the migratory insertion occurs from a five-coordinate *intermediate*. This d^8 intermediate could have a trigonal bipyramidal structure, as drawn here, but another likely alternative is a square pyramid. We could not exclude, following the work of Garrou and Heck,[3c] a third possibility in which these two routes are linked at a five-coordinate structure $[Pd(NH_3)_3(CH_3)(CO)]^+$. The dissociation of one amine ligand from this structure could then lead to the four-coordinate carbonyl complex of the dissociative route. Note, however, that, at variance with Garrou and Heck, we do not make any assumption in this case as to whether this five-coordinate structure is an intermediate or a transition state.

In order to discriminate between these various possibilities we first optimized the structures **I–XI** at the SCF level. Electron-correlation effects were then taken into account by performing MP2 calculations on these SCF-optimized structures (hereafter denoted MP2// SCF). Structures **I–VI** are involved in the dissociative route (Scheme 2), **IV** being the transition state for the CO insertion step. Structures **VII–XI** (Scheme 3) pertain to the two other routes. It is important to note here that **VIII** and **X** are found to be transition states and not intermediates on the potential-energy hypersurface of the $\{[Pd(CH_3)(NH_3)_3]^+ + CO\}$ composite system. The bond distances and angles are collected in Table 4, and the relative SCF and MP2 energies are given in Table 5.

In addition to and in order to check the validity of the MP2 calculations, CAS–SCF and CAS–SCF/CI calculations were carried out for the NH_3 dissociation step on the structures **I** and **II**···NH_3 (Pd···NH_3 = 100 Å, Table 6) and on the structures **III** and **V** of the CO insertion step (Table 7).

Table 4. Calculated Bond Distances and Angles of Structures I–XIII

structure	Bond Distances (Å)						
	Pd–N¹	Pd–N²	Pd–N³	Pd–C¹	Pd–C²	C¹–C²	C²–O
I	2.184	2.275	2.182	2.048			
II	2.247	2.253		1.995			
III	2.182	2.265		2.056	2.106		1.125
IV	2.214	2.248		2.436	1.888	1.897	1.153
V	2.241	2.252			1.962	1.521	1.193
VI	2.235	2.180	2.167		2.054	1.521	1.224
VII	2.183	2.266	2.187	2.047	3.371		1.133
VIII	2.316	2.269	2.539	2.019	2.399		1.129
IX	2.216	2.268	2.841	2.049	2.128		1.126
X	2.175	2.870	2.175	2.044	2.732		1.130
XI	2.198	3.181	2.198	2.032	2.250		1.128
XIII	2.215	2.278	2.782	2.419	1.884	1.929	1.154

structure	Bond Angles (deg)					
	N¹–Pd–N²	N¹–Pd–C¹	N¹–Pd–N³	N²–Pd–C¹	N²–Pd–N³	N³–Pd–C¹
I	92.14	87.83	175.48	178.07	91.80	88.16
II	98.02	89.31		172.64		
III	92.59	87.69		178.37		
IV	95.73	111.67		152.60		
V	99.88					
VI	90.32		90.47		179.12	
VII	91.87	88.13	176.08	179.47	91.83	88.15
VIII	90.81	89.78	125.00	179.41	89.53	90.13
IX	92.29	87.96	93.00	177.51	87.60	94.86
X	92.16	88.57	175.67	131.26	92.17	88.57
XI	93.75	88.74	172.50	109.68	93.75	88.74
XIII	95.32	110.54	92.06	153.19	92.03	93.93

intermediate	Bond Angles (deg)					
	C¹–Pd–C²	N¹–Pd–C²	N²–Pd–C²	N³–Pd–C²	Pd–C²–O	Pd–C²–C¹
I						
II						
III	85.62		94.04	173.00	179.97	
IV	50.10	161.77	102.50		157.28	80.11
V		171.34	88.78		127.77	103.25
VI		176.73	92.90	86.32	117.25	123.68
VII	92.01	89.56	87.46	89.30	184.85	
VIII	90.18	144.29	89.34	90.71	179.32	
IX	85.79	169.30	93.59	96.17	178.61	
X	155.22	90.61	73.51	90.62	177.33	
XI	180.74	91.31	69.58	91.31	174.03	
XIII	51.45	161.94	102.40	90.82	159.51	78.73

Table 5. Calculated SCF and MP2 Energies (kcal mol⁻¹) of Structures I–XIII[a]

structure	energy	structure	RHF
I	0	VII	−3.1 (−5.6)
II	35.0 (42.2)	VIII	6.0 (1.7)
III	14.2 (7.0)	IX	4.1 (−4.6)
IV	41.2 (25.8)	X	8.1
V	15.8 (12.7)	XI	4.8
VI	−16.1 (−16.1)	XIII	23.5 (16.3)

[a] All energies are relative to the energy of intermediate I + CO. MP2//SCF values are in parentheses.

Table 6. Comparison of the Energy Differences (kcal mol⁻¹) between Structures I and II (Scheme 2) as a Function of the Calculational Method

method	ΔE	method	ΔE
RHF	35.0	CAS–SCF	30.0
MP2	42.2	SD–CI+Q	31.9

Table 7. Dependency of the Relative Energy Values (kcal mol⁻¹) of the Process II → III → IV on the Calculational Method and the Type of Complex

method	reactant	TS	product
RHF	0.0	27.0	1.6
MP2	0.0	18.8	5.7
CAS–SCF	0.0		6.2
SD–CI	0.0		1.2
SD–CI+Q	0.0		−1.4

Discussion

Carbonylation of Organopalladium(II) Cations and NMR Studies.

The insertion of carbon monoxide into the palladium–carbon bond of the complexes bearing tridentate ligands occurs easily. Most of the insertion products are much more stable toward decarbonylation than the acylpalladium(II) complexes of mono- or bidentate ligands. The reaction is reversible under forcing conditions and can, in most cases, be repeated several times at room temperature without significant loss of the parent complex involved.

For most of the complexes carbonylation is complete within 2.5 min at 10 atm of CO in CD₃COCD₃. Only the complexes with a mesityl (**1f** and **2,3e**) or a 4-nitrophenyl group (**1c** and **2,3d**) react slower, and some of these do not even fully carbonylate under these conditions. The carbonylation under high CO pressure is much faster than our earlier reported results at atmospheric pressure, *i.e.*, under the latter conditions the complex [PdPh(NN'N)]OTf (**1b**) reacts about 6 times faster with CO (30 min) than the 1-naphthyl analog **1e** (3 h).[8] These differences were attributed to the larger bulk of the 1-naphthyl group with respect to the phenyl group. The fast insertion under high CO pressure is a

Scheme 4

Scheme 5

C—N = [structure: phenyl with —NMe₂]
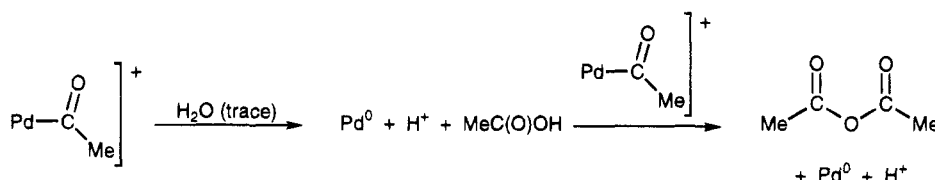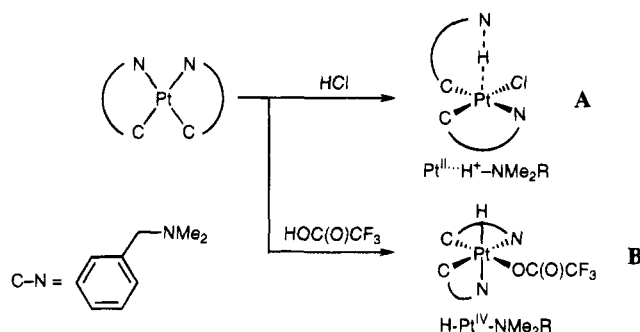
consequence of the higher CO concentration in solution, but the mixing of CO into the solution is a limiting factor. This is supported by an experiment in which [PdPh(NN′N)]OTf (**1b**) was added in one portion as a solid to an acetone solution saturated with CO at 1 atm. This resulted in instantaneous CO insertion. The conversion times given in Table 2 therefore do not have more than a qualitative value.

The stability of the CO inserted products depends on the nature of the tridentate ligand. Whereas all three ligands give aroyl complexes that can be characterized and in most cases isolated as stable solids, only the pmdeta and pico lignds allow isolation of their acetyl complexes. The surprising formation of acetic anhydride upon the CO insertion in [PdMe(NN′N)]OTf (**1a**, eq 2) is probably due to the presence of trace amounts of water in the solvent (CD₃COCD₃ or methylene chloride). A possible reaction path to acetic anhydride is presented in Scheme 4. It is based on the intermediacy of an acetylpalladium species, and it is proposed that the acetic anhydride is formed by attack of acetic acid on this acetyl intermediate.

The conversion of the acyl group into acetic acid can be rationalized on the basis of our earlier observation of tautomeric products **A** and **B** in the protonation of bis-*C,N*-chelated platinum complexes (Scheme 5).[18] We presume that in the present case the water acts as a nucleophile leading to the tautomeric structures **C** [Pd^{II}(acyl)(water)] and/or **D** [Pd^{IV}(acyl)(hydride)(hydroxyl)].

Although the linear N—H⋯Pt arrangement in **A** cannot be attained by **C**, the similarity is evident. The formation of **D** requires only a small geometrical change of the N, H, and OH ligands in **C** to give formally a palladium(IV) center, *i.e.*, an oxidative addition of water to palladium(II). The C—OH bond may then be formed by a reductive elimination from **D** or a nucleophilic

C   D
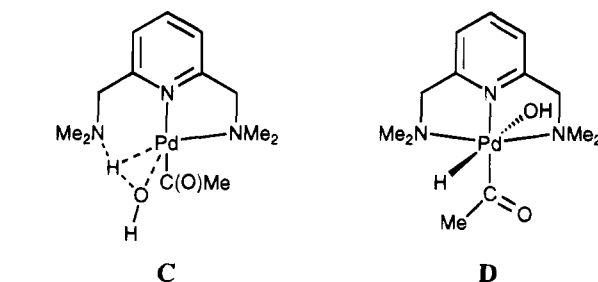
addition (intramolecularly or by a second water molecule assisted by the Pd—OH bond). To our knowledge, there are very few examples of reactions of palladium complexes with water, probably due to the low polarizability of the Pd—C bond.[19] Because of the higher electrophilicity of palladium(II) cations, reaction with water may be more facile. The difference in this respect between the NN′N complex and the pico/pmdeta complexes is not yet understood.

Ab Initio Studies on the Carbonylation Mechanism.
A look at the Table 4 indicates that most of the calculated bond distances and bond angles are within reasonable range of those obtained from X-ray molecular structures for similar systems.[20] Also the geometry of the transition state **IV** is quite close to the one reported by Koga and Morokuma[2e] for the CO insertion into the Pd—CH₃ bond of the neutral [Pd(PH₃)(H)(CH₃)(CO)] system despite the use of a different basis set. (In fact, pilot calculations which we carried out on the reaction **III** → **IV** → **V** indicated that the corresponding geometries are not very sensitive to the quality of the basis set.) The most noticeable exceptions are for the apical bonds of the intermediates with five surrounding groups, **VII** (Pd—C² = 3.371Å), **IX** (Pd—N³ = 2.841Å), and **XI** (Pd—N² = 3.181Å). Thus these intermediates had rather be viewed as square planar Pd complexes weakly interacting with a fifth moiety. The interaction is particularly weak for **VII**, which is computed at the SCF level to be more stable than **I** + CO by only 3.1 kcal mol⁻¹. The MP2 calculations increase this stabilization to 5.6 kcal mol⁻¹ (SCF-optimized geometry), but one should subtract from this value the basis set superposition error which is estimated (at the SCF level using

(18) (a) Wehman-Ooyevaar, I. C. M.; Grove, D. M.; van der Sluis, P.; Spek, A. L.; van Koten, G. *J. Chem. Soc., Chem. Commun.* **1990**, 1367. (b) Wehman-Ooyevaar, I. C. M.; Grove, D. M.; Kooijman, H.; van der Sluis, P.; Spek, A. L.; van Koten, G. *J. Am. Chem. Soc.* **1992**, *114*, 9916. (c) Wehman-Ooyevaar, I. C. M.; Grove, D. M.; de Vaal, P.; Dedieu, A.; van Koten, G. *Inorg. Chem.* **1992**, *31*, 5484. (d) Pregosin, P. S.; Rüegger, H.; Wombacher, F.; van Koten, G.; Grove, D. M.; Wehman-Ooyevaar, I. C. M. *Magn. Reson. Chem.* **1992**, *30*, 548.

(19) See for example: (a) Vicente, J.; Abad, J.-A.; Gil-Rubio, J.; Jones, P. G.; Bembenek, E. *Organometallics* **1993**, *12*, 4151. (b) Canty, A. J.; Honeyman, R. T.; Roberts, A. S.; Traill, P. R.; Colton, R.; Skelton, B. W.; White, A. H. *J. Organomet. Chem.* **1994**, *471*, C8. (c) Valk, J. M.; van Belzen, R.; Kooijman, H.; Spek, A. L.; Boersma, J.; van Koten, G. Manuscript in preparation.

(20) (a) de Graaf, W.; Harder, S.; Boersma, J.; van Koten, G.; Kanters, J. A. *J. Organomet. Chem.* **1988**, *358*, 545. (b) de Graaf, W.; Boersma, J.; Smeets, W. J. J.; Spek, A. L.; van Koten, G. *Organometallics* **1989**, *8*, 2907. (c) Alsters, P. L.; Baesjou, P. J.; Janssen, M. D.; Kooijman, H.; Sicherer-Roetman, A.; Spek, A. L.; van Koten, G. *Organometallics* **1992**, *11*, 4124. (d) Alsters, P. L.; Boersma, J.; Smeets, W. J. J.; Spek, A. L.; van Koten, G. *Organometallics* **1993**, *12*, 1639. (e) Alsters, P. L.; Engel, P. F.; Hogerheide, M. P.; Copijn, M.; Spek, A. L.; van Koten, G. *Organometallics* **1993**, *12*, 1831. (f) Markies, B. A.; Canty, A. J.; de Graaf, W.; Boersma, J.; Janssen, M. D.; Hogerheide, M. P.; Smeets, W. J. J.; Spek, A. L.; van Koten, G. *J. Organomet. Chem.* **1994**, *482*, 191.
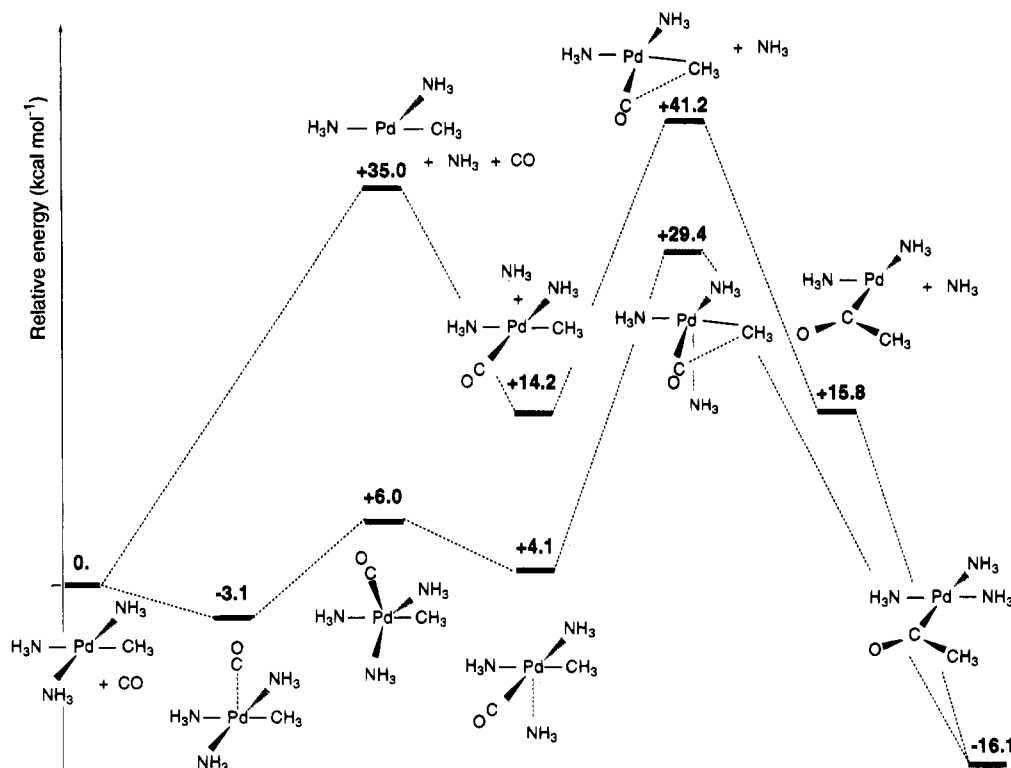
Figure 3. Energy profiles (SCF level) of the cationic system.

the counterpose method) to be 4.6 kcal mol⁻¹. In **IX**, the stabilization of [Pd(NH₃)₂(CH₃)(CO)]⁺ by the association with NH₃ is somewhat larger: 10.1 kcal mol⁻¹ at the SCF level and 11.6 kcal mol⁻¹ at the MP2//SCF level. It should not be offset by the basis set superposition error which we estimate to be less than 6–7 kcal mol⁻¹.[21] In line with these results one gets a shorter apical bond length in **IX**, see Table 4. Like in the naked Pd(NH₃) system recently computed by Blomberg *et al.*,[22] the interaction energy may involve an electron nuclear attraction between the lone pair and the palladium core. It may also be simply the result of some electrostatic attraction between the dipole of the NH₃ molecule and the positive charge of the cationic [Pd(NH₃)₂(CH₃)(CO)]⁺ entity.

It should be stressed here that the optimization procedures never led to trigonal bipyramidal (TBP) intermediates. Distorted TBP structures, **VIII** and **X**, were instead found and characterized as *transition states* for NH₃ substitution by CO. In these structures the N¹–Pd–N³ angle is close to 180°, but the angle between the CO incoming group and the NH₃ leaving group is much smaller than 120°. A similar feature has been already recognized by Lin and Hall in square planar Pt(II) and Rh(I) substitution reactions, and they ascribe it to the minimization of the repulsion between the electron concentration on the central atom and the electron concentration on the entering and leaving ligands.[23] In both cases the angle between CO and the spectator equatorial ligand (either NH₃ or CH₃) is quite large (144° in **VIII** and 155° in **X**). This reflects the

(21) A counterpoise calculation carried out for a similar geometry but with the two NH₃ ligands trans to each other and a Pd–N$_{axial}$ bond length of 2.48 Å yielded a basis set superposition error of 6.7 kcal mol⁻¹. The longer Pd–N$_{axial}$ bond in **IX** (2.84 Å) should lead to a smaller error.

(22) Blomberg, M. R. A.; Siegbahn, P. E. M.; Svensson, M. *Inorg. Chem.* **1993**, *32*, 4218.

(23) Lin, Z.; Hall, M. B. *Inorg. Chem.* **1991**, *30*, 646.

late nature of these two transition states, *i.e.*, they are product-like, as expected from the endothermicity computed for the NH₃ substitution by CO (*vide infra*). Finally the larger trans influence of CH₃ compared to NH₃ is best seen in the comparison of the lengths of the equatorial Pd–NH₃ bond that is trans either to NH₃ (2.539 Å in **VIII**) or to CH₃ (2.870 Å in **X**).

Thus it seems from these results that, at least in the gas phase, a purely associative pathway (*i.e.*, involving intermediates with five ligands *firmly* attached to the central atom and in which the CO insertion step takes place) can be ruled out for the cationic palladium complexes. Another possible candidate for a five-coordinate intermediate, *i.e.*, **XII**, is not a local minimum since its optimization led directly to **XI**.

We are therefore left with two alternative pathways for the carbonylation process: either a dissociative pathway involving the three coordinate [Pd(NH₃)₂-(CH₃)]⁺ system as a key intermediate or a hybrid pathway where the associative nature of the mechanism is essentially limited to the amine substitution step. The two corresponding energy profiles are shown in Figure 3 (SCF values).

The MP2 calculations lead to overall conclusions that are similar to the ones obtained at the SCF level (*vide infra*), and we will therefore base our discussion mostly on the SCF values.

Dissociative Pathway. The formation of the transition state **IV** (+41.2 kcal mol⁻¹, SCF value) appears to be the rate-determining step and not the dissociation of NH₃ from the initial [Pd(NH₃)₃(CH₃)]⁺ cation (+35 kcal mol⁻¹, SCF value), whatever the level of calculation is, see the Tables 6 and 7. It should be noted that the MP2 calculations overestimate the binding of NH₃: the NH₃ bond dissociation energy increases from 35 to 42.2 kcal mol⁻¹, whereas CAS–SCF/CI calculations lead to a slight decrease from 35 to 31.9 kcal mol⁻¹. The

thermodynamics of the insertion step is also less favorable at the MP2 level ($+5.7$ kcal mol^{-1}) than at the CAS−SCF level (-1.4 kcal mol^{-1}). This corresponds to the result that we obtained some years ago for the model reaction [Pd(H)(CO)]$^+$ → [Pd(CHO)]$^+$.[3h] In contrast, the inclusion of correlation leads to a decrease of the energy barrier between **III** and **IV**: the MP2 value is 18.8 kcal mol^{-1}. CAS−SCF/CI calculations are expected to give a value similar to the MP2 value: pilot calculations which were carried out for a structure quite close to the transition state yielded MP2 and CAS−SCF/CI values differing by only 0.5 kcal mol^{-1}.[24] Thus the decrease of the energy barrier obtained at the MP2 level is probably meaningful.

Since **IV** is coordinatively unsaturated, one may wonder whether a η^2 structure might be more stable. We find such a structure, see **V'**, as a local minimum.


V'
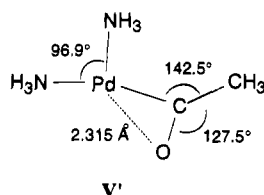
However, the Pd−O bond distance of 2.315 Å points to a rather weak Pd−O interaction. Moreover, **V'** is found to be more stable than **V** by only 2.6 kcal mol^{-1} at the SCF level and *destablized* by 0.4 kcal mol^{-1} at the MP2 level. Thus the recombination of the dissociated amine to yield the final four-coordinate acyl product is energetically favored.

Hybrid Pathway. The high energy required for the dissociation of NH$_3$ from [Pd(NH$_3$)$_3$(CH$_3$)]$^+$ makes a purely dissociative pathway rather unlikely. In fact the NH$_3$ substitution by CO turns out to be easier when going through the five-coordinate *transition state* **VIII**. The energy barrier from **I** + CO is computed to be 6.0 kcal mol^{-1} only at the SCF level. MP2 calculations even lower this value to 1.7 kcal/mol. The MP2 value may be too low owing to some overestimation of the metal−carbonyl bond energy.[25,26] In **VIII**, the NH$_3$ ligand cis to CH$_3$ is slightly elongated (by 0.36 Å) and the N^1−Pd−N^3 angle amounts to 125°. The tridendate nitrogen donor ligands should be able to achieve this arrangement: we note that in the crystal structures of [Pd(Me)-(NN'N)]$^+$,[9] [Pd(COC$_{10}$H$_7$)(NN'N)]$^+$, and [Pd(C$_6$H$_4$-o-C$_7$H$_{11}$)(pmdeta)]$^+$,[27] the N^1−Pd−N^3 angle is much smaller than 180°, ranging from 159.7 to 165.5°. These systems are therefore deformed in the right direction, and the substitution step should likely proceed through a transition state analogous to **VIII**. Another transition state for the CO/NH$_3$ substitution might be **X**, but this one is slightly higher in energy than **VIII** (by 2.1 kcal mol^{-1}). Moreover, the nitrogen atom which is pushed away from the metal in this transition state is the one correspond-

ing to the central atom of the tridentate ligands that evidently cannot dissociate in the actual system.

We have already mentioned that before and after the transition state there might be some stabilization of the four-coordinate intermediates by the incoming CO and the leaving NH$_3$, respectively. However, the stabilization by CO, if any, is very weak (*vide supra*). The stabilization by NH$_3$ is greater. Interestingly too, the presence of NH$_3$ in the vicinity of the Pd coordination sphere also stabilizes the transition state of the insertion step through a loose association, see **XIII**.

XIII
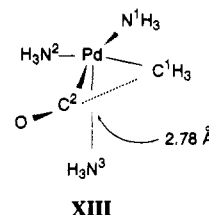
The barrier for the insertion in the presence of ammonia is computed to be 23.5 kcal mol^{-1} at the SCF level. Electron correlation again lowers this barrier, bringing it down to 16.3 kcal mol^{-1} at the MP2 level. The stabilization of the transition state is slightly greater than the stabilization of the four-coordinate carbonyl complex (at both SCF and MP2//SCF levels). Although this differential effect is quite small, it is corroborated by the change in the Pd−NH$_3$ distance, 2.78 vs. 2.84 Å. The effect might be greater with a ligand that is more basic than NH$_3$, such as the tertiary amine end of the pico or pmdeta terdentate ligands, thus providing some sort of nucleophilic catalysis for the insertion. Alternatively acetone, which is a coordinating solvent, might provide the same type of catalysis. The fact that nucleophiles can catalyze the formation of coordinatively unsaturated acyl intermediates has been already recognized experimentally for the CO insertion in some manganese aryl complexes.[28] The strong exothermicity computed for the formation of the four-coordinate acyl product and the presence of the dissociated amine in the vicinity of the coordination sphere might well drive the system directly to this final acyl product, as depicted in Figure 3.[29]

Comparison with the Neutral System. In order to shed some more light on the comparison between the ionic and the neutral system, similar calculations were performed on the neutral {*trans*-[Pd(NH$_3$)$_2$(CH$_3$)$_2$] + CO} system, obtained by replacing the NH$_3$ ligand trans to the migrating methyl by a CH$_3$ group. The corresponding results are summarized in Figure 4 (SCF values only, the MP2//SCF calculations yielding again the same overall conclusions).

As for the cationic system the dissociative pathway is not favored. Instead, the NH$_3$ substitution by CO takes place associatively and the five-coordinate transition state lies 7 kcal mol^{-1} above the reactants (MP2 calculations lower this value down to 2.9 kcal mol^{-1}). In contrast to the ionic system, the five-coordinate equilibrium structures which have either CO or NH$_3$

(24) This structure was obtained by using the $C_{Me}-C_{CO}$ distance as a reaction coordinate carrying out a gradient optimization for discrete points of this reaction coordinate and then performing a quadratic interpolation of the energies of the corresponding geometries. The structure obtained through this procedure was found to be quite similar to the transition state structure except for the Pd−C_{Me} bond length, which was too short by 0.15 Å.

(25) Rohlfing, C.; Hay, P. J. *J. Chem. Phys.* **1985**, *83*, 4641.

(26) Ehlers, A. W.; Frenking, G. *J. Am. Chem. Soc.* **1994**, *116*, 1514.

(27) Markies, B. A.; Wijkens, P.; Kooijman, H.; Spek, A. L.; Boersma, J.; van Koten, G. *J. Chem. Soc., Chem. Commun.* **1992**, 1420.

(28) Webb, S. L.; Giandomenico, C. M.; Halpern, J. *J. Am. Chem. Soc.* **1986**, *108*, 345.

(29) In that sense the reaction profile would look like the reaction profile expected for the associative mechanism. The difference here is that at least one ligand (either CO or NH$_3$) stays quite distant from the metallic center.
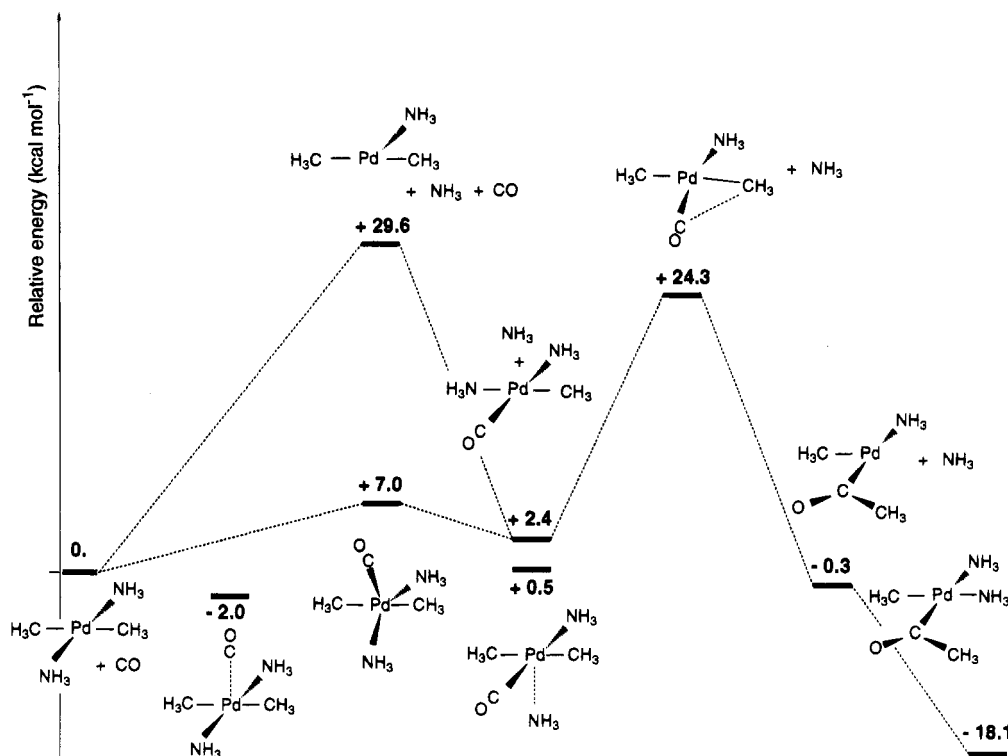
Figure 4. Energy profiles (SCF level) of the neutral system.

loosely bound at the apex of the square pyramid are hardly stabilized with respect to their dissociated counterparts, the interaction energy being only 2 kcal mol^{-1}. The Pd$\cdots$CO and Pd$\cdots$NH$_3$ distances (3.36 and 3.11 Å, respectively) are also much larger than in the ionic case. Thus these structures are most likely artefacts of the basis set superposition error and do not correspond to actual intermediates in the substitution process.

We were also unable to find an equilibrium structure for a transition state which has the NH$_3$ ligand in the vicinity of the coordination sphere. The optimized transition state corresponds therefore to the reaction taking place in the square planar [Pd(NH$_3$)(CH$_3$)$_2$(CO)] complex. The associated barrier is computed to be 21.9 kcal mol^{-1} at the SCF level and 15.6 kcal mol^{-1} at the MP2//SCF level, i.e., slightly lower at both levels than the barrier in the [Pd(NH$_3$)$_2$(CH$_3$)(CO)]$^+$ ionic system. Moreover, both the insertion step and the overall process are more exothermic in the neutral system. Thus the greater reactivity of the cationic systems which is observed experimentally,[6d,g] does not seem to be an intrinsic property of the cationic character, at least in the gas phase. The lowering of the energy barrier might well result from a difference in the trans influence of the ligand sitting trans to the migrating group: the neutral system mentioned above has a trans CH$_3$ group instead of the trans NH$_3$ ligand present in the cationic system. To test this hypothesis we have also determined the energy barrier for the insertion process in the [Pd(Cl)(NH$_3$)(CH$_3$)(CO)] system with the chlorine ligand either cis or trans to the CH$_3$ migrating group. As seen from Table 8 the energy barrier in this neutral system is greater than the barrier in the cationic [Pd-(NH$_3$)$_2$(CH$_3$)(CO)]$^+$ system.

Finally one should not overlook differential solvation effects. Solvation effects might be greater for the cationic system than for the neutral one. In particular,

Table 8. Energy Barrier (MP2//SCF Value, in kcal mol^{-1}) for the CO Insertion into the Pd-CH$_3$ Bond of Various Cationic and Neutral Square Planar Complexes

system	$\Delta E^{\ddagger}_{insertion}$
$\begin{array}{c} NH_3 \\ H_3N-Pd-CH_3 \\ CO \end{array}\Big]^+$	18.8
$\begin{array}{c} NH_3 \\ H_3C-Pd-CH_3 \\ CO \end{array}$	15.4
$\begin{array}{c} NH_3 \\ Cl-Pd-CH_3 \\ CO \end{array}$	21.2
$\begin{array}{c} Cl \\ H_3N-Pd-CH_3 \\ CO \end{array}$	22.3

a coordinating solvent such as acetone with its oxygen lone pair might catalyze more efficiently the insertion step in the cationic system. Calculations are presently under way to test this hypothesis.

Direct Insertion of CO. It has been suggested from calculations carried out on the PdCH$_3$ + CO system that CO might well insert directly into the Pd–C bond without prior coordination to the palladium center.[3m] We do not find any transition state corresponding to this behavior in our calculations. Structure **X**, which has the CO and CH$_3$ ligands cis to each other, is not a transition state for a direct CO insertion, according to both its geometry (the C^1–Pd–C^2 angle is quite obtuse) and the eigenvector corresponding to the negative eigenvalue of the Hessian matrix, but is instead the transition state between **VII** and **XI**. Moreover, an attempt to locate a transition state corresponding to the

direct insertion resulted in a structure with a coordinated acetyl ligand lying perpendicularly to the Pd–N$_3$ plane. This structure, which lies 6.1 kcal mol^{-1} (SCF value) above **VI**, is therefore the transition state for the rotation of the acetyl ligand. Thus the perpendicular disposition of the aroyl ligand in Figure 1 should be traced to steric rather than to electronic requirements.

Concluding Remarks

We have shown that acetyl and aroyl cations containing the tridentate nitrogen-donor ligands *N*-(2-picolyl)-*N*,*N*′,*N*′-trimethylethylenediamine (pico) and *N*,*N*,*N*′,-*N*″,*N*″-pentamethyldiethylenetriamine (pmdeta) can be easily isolated, except for the 4-nitrophenyl and mesityl derivatives which decarbonylate upon attempted isolation. The aroyl complexes of the ligand 2,6-bis[(dimethylamino)methyl]pyridine (NN′N) can be observed using high-pressure NMR, but most of them decarbonylate upon attempted isolation except for the 1-naphthoyl derivative of which an X-ray molecular structure was obtained. Moreover, the pico and pmdeta complexes are all stable toward methanol, whereas the NN′N complexes immediately decompose in this solvent. The unexpected formation of acetic anhydride upon carbonylation of [PdMe(NN′N)]OTf with subsequent hydrolysis is a striking example of the ligand-dependent stability of the carbonylation products. Qualitative interpretation of NMR results shows that the carbonylation is influenced by (a) the ligand, (b) the size of the aryl moiety, and (c) the presence of strong electron-withdrawing groups in the aryl group.

The *ab initio* calculations on the system [Pd(CH$_3$)-(NH$_3$)$_3$]$^+$ + CO did provide, however, more insight into the carbonylation mechanism as well as into the differences between neutral and ionic palladium(II) complexes. According to our calculations, a purely dissociative mechanism should not be expected to occur as the Pd–N bond dissociation is found to be a high-energy process. The calculations also show that strong CO coordination to give a five-coordinate complex is not feasible in the chosen model system and that a purely associative CO insertion process is thus unlikely to occur. Nevertheless, a five-coordinate complex occurs as a *transition state* in the concerted ligand exchange of NH$_3$ for CO, which appeared to be a low-energy process. According to the energy profiles (Figures 3 and 4), this step should always be faster than the CO insertion step. Thus, irrespective of the nature of the palladium species (neutral or cationic), the migratory insertion and not the ligand substitution is the rate-determining step in the carbonylation process. Moreover, because of the low-energy pathway for substitution of a NH$_3$ for a CO ligand, the overall process should be independent of the CO pressure. This is corroborated by the experimental results. The overall process is highly dependent on the overall difference between these two barriers, the first being more sensitive to steric factors, *i.e.*, to the structure of both the tridentate N-donor ligand and the aryl group. This explains the incoherent results of the carbonylation reaction under different circumstances as well as the lower carbonylation rate found for sterically hindered aryls. Most interestingly, the insertion seems to be assisted by the dissociated amine which is kept in the vicinity of the coordination sphere. The solvent might play a similar

role. The relative energetics of the neutral and the cationic system, although similar, seem to depend on the ligand environment, at least for the gas-phase species investigated here. The greater reactivity of the ionic system which is experimentally observed might also be due to a greater solvent assistance. These features are currently being explored. The model system used here, and possible variations of it, can be expected to provide good leads to more insight into the basic steps of insertion-type reactions. The reactivity of these cationic complexes toward other nucleophilic reagents, *i.e.*, alkenes, has also been explored.[27]

Experimental Section

All procedures were carried out in standard Schlenk-type glassware. The alkyl- and arylpalladium complexes were prepared using established methods.[6b] Acetone (p.A.) was obtained from Janssen Chimica, and CD$_3$COCD$_3$ was obtained from ISOTEC Inc.; both solvents were used without further purification. ^{1}H (200 or 300 MHz) and ^{13}C (50 or 75 MHz) NMR spectra were recorded on Bruker AC200 or AC300 spectrometers in air at 1 atm pressure and ambient temperature unless noted otherwise. Chemical shifts (δ) are given in ppm relative to tetramethylsilane, and coupling constants are presented in Hz. Accurate chemical shifts and coupling constants for conformational analyses were obtained using IvorySoft's geNMR simulation program (version 3.4 for MS-DOS). FTIR spectra were obtained on a Mattson Galaxy 5000 spectrometer. GLC analyses were performed on a Philips PU4600 gas chromatograph equipped with a capillary column (DB17, J&W Scientific). The GCMS analyses were performed by the Department of Mass Spectrometry, Utrecht University, The Netherlands. Elemental analyses were performed by Dornis u. Kolbe, Mülheim a. d. Ruhr, Federal Republic of Germany.

Synthesis and Characterization of the Acetyl and Aroyl Complexes. All isolated complexes were prepared using the following typical procedure: Carbon monoxide (1 atm) was bubbled through a solution of 0.10 g (0.2 mmol) [PdPh(pmdeta)]OTf (**3b**) in acetone (5 mL) for 1 min. The vessel was then closed, and the solution was stirred for 1 h. Subsequently, the solution was filtered through filter-aid, and the volatiles evaporated *in vacuo*. The residue was recrystallized from methanol/diethyl ether to give 0.10 g (95%) of yellow crystalline [Pd(COPh)(pmdeta)]OTf (**6b**). Most complexes could also be recrystallized from acetone/pentane. IR spectra of the unstable complexes were obtained by rapid precipitation of the complexes from CD$_3$COCD$_3$ solution by addition of a large volume of pentane, except for **4c** which decarbonylated too quickly upon pressure release.

(Benzoyl){2,6-bis[(dimethylamino)methyl]pyridine}-palladium Trifluoromethanesulfonate (4b). ^{1}H NMR (200 MHz, CD$_3$COCD$_3$, δ): 2.79 (s, 12, NMe$_2$); 4.53 (s, 4, CH$_2$); 7.58 (m, 3, Ph[3,4,5]); 7.64 (d, ^3J = 7.8, 2, Py[3,5]); 8.14 (t, 2 × ^3J = 7.8, 1, Py[4]); 8.42 (m, 2, Ph[2,6]). ^{13}C NMR (50 MHz, CD$_3$COCD$_3$, 10 atm of CO, δ): 52.48 (NMe$_2$); 72.86 (CH$_2$); 122.11 (Py[3,5]); 129.72, 130.03, 133.00, 136.57 (Ph); 141.78 (Py[4]); 156.30 (Py[2,6]); 237.26 (CO). IR (KBr): 1626 cm^{-1}.

(4-Nitrobenzoyl){2,6-bis[(dimethylamino)methyl]-pyridine}palladium Trifluoromethanesulfonate (4c). ^{1}H NMR (200 MHz, CD$_3$COCD$_3$, 25 atm of CO, δ): 2.81 (s, 12, NMe$_2$); 4.56 (s, 4, CH$_2$); 7.65 (d, ^3J = 7.8, 2, Py[3,5]); 8.15 (t, 2 × ^3J = 7.8, 1, Py[4]); 8.40 (m, 2, Py[3,5]); 8.67 (m, 2, Py[2,6]).

(2-Methyl-1-benzoyl){2,6-bis[(dimethylamino)methyl]-pyridine}palladium Trifluoromethanesulfonate (4d). ^{1}H NMR (200 MHz, CD$_3$COCD$_3$, δ): 2.53 (s, 3, Me-tolyl); 2.72 (s, 12, NMe$_2$); 4.48 (s, 4, CH$_2$); 7.25 (m, 1, Ph); 7.45 (m, 2, Ph); 7.61 (d, ^3J = 7.8, 2, Py[3,5]); 8.11 (t, 2 × ^3J = 7.8, 1, Py[4]); 8.91 (m, 1, Ph). ^{13}C NMR (50 MHz, CD$_3$COCD$_3$, δ): 20.75 (Me-tolyl); 51.90 (NMe$_2$); 72.56 (CH$_2$); 122.08 (Py[3,5]); 123.60,

127.00, 131.57, 131.96, 134.44, 136.15 (Ph); 141.79 (Py[4]); 156.18 (Py[2,6]), 237.24 (CO). IR (KBr): 1630 cm^{-1}.

(1-Naphthoyl){2,6-bis[(dimethylamino)methyl]-pyridine}palladium Trifluoromethanesulfonate (4e). Recrystallization could only be performed from acetone/pentane under a CO atmosphere. Yield: 86%. Mp: 142 °C (decomp). ^{1}H NMR (200 MHz, CD$_3$COCD$_3$, 10 atm of CO, δ): 2.75 (s, 12, NMe$_2$); 4.52 (s, 4, CH$_2$); 7.62 (m, 4, naphthyl + Py[3,5]); 7.79 (m, 1, naphthyl); 8.01 (m, 1, naphthyl); 8.14 (m, 2, naphthyl + Py[4]); 8.83 (m, 1, naphthyl); 9.31 (m, 1, naphthyl). ^{13}C NMR (50 MHz, CD$_3$COCD$_3$, 10 atm of CO, δ): 52.02 (NMe$_2$); 72.65 (CH$_2$); 122.15 (Py[3,5]); 126.10, 126.28, 127.46, 128.35, 129.11, 132.92, 133.40, 134.70, 135.47 (naphthyl); 141.85 (Py[4]); 156.35 (Py[2,6]); CO not observed. IR (KBr): 1610 cm^{-1}. Anal. Calcd for C$_{23}$H$_{24}$N$_3$F$_3$O$_4$PdS: C, 45.59; H, 4.66; N, 6.93. Found: C, 45.82; H, 4.49; N, 7.10.

(2,4,6-Trimethylbenzoyl){2,6-bis[(dimethylamino)-methyl]pyridine}palladium Trifluoromethanesulfonate (4f). ^{1}H NMR (200 MHz, CD$_3$COCD$_3$, 25 atm of CO, δ): 2.28 (s, 3, Me-mesityl); 2.66 (s, 6, NMe$_2$); 2.72 (s, 3, Me-mesityl); 2.96 (s, 3, Me-mesityl); 4.42 (s, 4, CH$_2$); 6.95 (s, 2, mesityl); 7.62 (d, ^3J = 7.8, 2, Py[3,5]); 8.12 (t, 2 × ^3J = 7.8, 1, Py[4])). IR (KBr): 1643 cm^{-1}.

(Acetyl){N-(2-picolyl)-N,N′,N′-trimethylethylene-diamine}palladium Trifluoromethanesulfonate (5a). Yield: 89%. Mp: 122 °C (decomp). ^{1}H NMR (300 MHz, CD$_3$COCD$_3$, δ): 2.52 (s, 3, NMe); 2.86 (m, ABXY, 1, CH$_2$CH$_2$-eq); 2.88 (m, ABXY, 1, CH$_2$CH$_2$-eq); 3.08 (s, 6, NMe$_2$); 3.56 (m, ABXY, 1, CH$_2$CH$_2$-ax); 3.70 (m, ABXY, 1, CH$_2$CH$_2$-ax); 4.11 (d, AX, ^2J = 15.1, 1, CH$_2$); 4.80 (d, AX, ^2J = 15.1, 1, CH$_2$); 7.59 (m, 1, Py); 7.71 (m, 1, Py); 8.15 (m, 2, Py). ^{13}C NMR (50 MHz, CD$_3$COCD$_3$, δ): 32.72 (CO*Me*); 42.13 (NMe); 50.24, 52.90 (NMe$_2$); 56.52, 64.86, 66.99 (CH$_2$); 125.84, 126.30, 141.20, 152.25, 164.07 (Py); 236.77 (CO). IR (KBr): 1676 cm^{-1}. Anal. Calcd for C$_{14}$H$_{22}$N$_3$F$_3$O$_4$PdS: C, 34.19; H, 4.51; N, 8.54. Found: C, 34.13; H, 4.58; N, 8.57.

(Benzoyl){N-(2-picolyl)-N,N′,N′-trimethylethylene-diamine}palladium Trifluoromethanesulfonate (5b). Yield: 70%. Mp: 143–145 °C. ^{1}H NMR (200 MHz, CD$_3$COCD$_3$, δ): 2.63 (s, 3, NMe); 2.73 (s, 3, NMe$_2$); 2.94 (s, 3, NMe$_2$); 2.97 (m, ABXY, 1, CH$_2$CH$_2$-eq); 2.98 (m, ABXY, 1, CH$_2$CH$_2$-eq); 3.72 (m, ABXY, 1, CH$_2$CH$_2$-ax); 3.84 (m, ABXY, 1, CH$_2$CH$_2$-ax); 4.24 (d, AX, ^2J = 15.3, 1, CH$_2$); 5.01 (d, AX, ^2J = 15.3, 1, CH$_2$); 7.39 (m, 1, Py[5]); 7.58 (m, 4, Ph[3,4,5] + Py[6]); 7.74 (d, ^3J = 7.8, 2, Py[3]); 8.09 (td, ^3J = 7.8, ^4J = 1.6, 1, Py[4]); 8.42 (m, 2, Ph[2,6]). ^{13}C NMR (50 MHz, CD$_3$COCD$_3$, δ): 42.38 (NMe); 50.07, 53.39 (NMe$_2$); 56.71, 64.97, 67.25 (CH$_2$); 125.82, 126.08 (Py[3,5]); 129.76 (Ph[3,5]); 130.68 (Ph[2,6]); 133.53 (Ph[4]); 136.34 (Ph[1]); 141.24 (Py[4]); 151.71 (Py[2]); 164.64 (Py[6]); 232.30 (CO). IR (KBr): 1638 cm^{-1}. Anal. Calcd for C$_{19}$H$_{24}$N$_3$F$_3$O$_4$PdS: C, 41.20; H, 4.37; N, 7.59. Found: C, 41.24; H, 4.45; N, 7.62.

(4-Methoxy-1-benzoyl){N-(2-picolyl)-N,N′,N′-trimethylethylenediamine}palladium Trifluoromethane-sulfonate (5c). Yield: 81%. Mp: 137 °C. ^{1}H NMR (300 MHz, CD$_3$COCD$_3$, δ): 2.63 (s, 3, NMe); 2.72 (s, 3, NMe$_2$); 2.93 (m, ABXY, 1, CH$_2$CH$_2$-eq); 2.94 (s, 3, NMe$_2$); 2.96 (m, ABXY, 1, CH$_2$CH$_2$-eq); 3.70 (m, ABXY, 1, CH$_2$CH$_2$-ax); 3.82 (m, ABXY, 1, CH$_2$CH$_2$-ax); 3.88 (s, 3, OMe); 4.21 (d, AX, ^2J = 15.2, 1, CH$_2$); 4.99 (d, AX, ^2J = 15.2, 1, CH$_2$); 7.03 (m, 2, Ph[3,5]); 7.40 (m, 1, Py[5]); 7.66 (m, 1, Py[6]); 7.73 (m, 1, Py[3]); 8.09 (m, 1, Py[4]); 8.40, (m, 2, Ph[2,6]). ^{13}C NMR (50 MHz, CD$_3$COCD$_3$, δ): 42.31 (NMe); 50.05, 53.36 (NMe$_2$); 56.01 (OMe); 56.67, 64.92, 67.17 (CH$_2$); 114.85 (Ph[3,5]); 125.78, 126.06 (Py[3,5]); 129.15 (Ph[1]); 132.92 (Ph[2,6]); 141.15 (Py[4]); 151.69 (Py[2]); 164.13 (Ph[4]); 164.62 (Py[6]); 229.66 (CO). IR (KBr): 1627 cm^{-1}. Anal. Calcd for C$_{20}$H$_{23}$N$_3$F$_3$O$_5$PdS: C, 41.35; H, 3.99; N, 7.23. Found: C, 41.22; H, 4.15; N, 7.29.

(4-Nitro-1-benzoyl){N-(2-picolyl)-N,N′,N′-trimethyl-ethylenediamine}palladium Trifluoromethanesulfonate (5d). ^{1}H NMR (200 MHz, CD$_3$COCD$_3$, 25 atm CO, δ): 2.67 (s, 3, NMe); 2.75 (s, 3, NMe$_2$); 2.90 (m, 2, CH$_2$CH$_2$-eq); 2.96 (s,

3, NMe$_2$); 3.82 (m, 2, CH$_2$CH$_2$-ax); 4.23 (d, AX, ^2J = 15.2, 1, CH$_2$); 5.13 (d, AX, ^2J = 15.2, 1, CH$_2$); 7.39 (m, 1, Py[5]); 7.66 (m, 1, Py[6]); 7.75 (m, 1, Py[3]); 8.10 (m, 1, Py[4]); 8.36 (m, 2, Ph[3,5]); 8.67 (m, 2, Ph[2,6]). ^{13}C NMR (50 MHz, CD$_3$COCD$_3$, 25 atm of CO, δ): 42.64 (NMe); 50.46, 53.31 (NMe$_2$); 56.77, 65.05, 67.51 (CH$_2$); 124.96 (Ph[3,5]); 125.83, 126.20 (Py[3,5]); 131.59 (Ph[2,6]); 140.27 (Ph[1]); 141.42 (Py[4]); 150.65 (Ph[4]); 151.88 (Py[2]); 164.84 (Py[6]); 232.85 (CO). IR (KBr): 1633 cm^{-1}.

(Acetyl){N,N,N′,N″,N″-pentamethyldiethylenetriamine}-palladium Trifluoromethanesulfonate (6a). Yield: 93%. Mp: 135 °C (decomp). ^{1}H NMR (300 MHz, CD$_3$COCD$_3$, 300 K, δ): 2.47 (s, 3, NMe); 2.67 (s, br, 6, NMe$_2$); 2.76 (s, 3, COMe); 2.87 (s, br, 6, NMe$_2$); 3.38 (m, ABXY, 2, CH$_2$CH$_2$-ax); 3.48 (m, ABXY, 2, CH$_2$CH$_2$-ax). ^{13}C NMR (50 MHz, CD$_3$COCD$_3$, δ): 30.53 (CO*Me*); 40.64 (NMe); 49.95, 53.73 (NMe$_2$); 57.03, 66.20 (CH$_2$); 240.79 (CO). IR (KBr): 1664 cm^{-1}. Anal. Calcd for C$_{12}$H$_{26}$N$_3$F$_3$O$_4$PdS: C, 30.55; H, 5.55; N, 8.91. Found: C, 30.56; H, 5.62; N, 8.84.

(Benzoyl){N,N,N′,N″,N″-pentamethyldiethylene-triamine}palladium Trifluoromethanesulfonate (6b). Yield: 95%. Mp: 146 °C. ^{1}H NRM (300 MHz, CD$_3$COCD$_3$, δ): 2.37 (s, 6, NMe$_2$); 2.74 (m, ABXY, 2, CH$_2$CH$_2$-eq); 2.83 (m, ABXY, 2, CH$_2$CH$_2$-eq); 2.91 (s, 6, NMe$_2$); 2.94 (s, 3, NMe); 3.57 (m, ABXY, 2, CH$_2$CH$_2$-ax); 3.58 (m, ABXY, 2, CH$_2$CH$_2$-ax); 7.58 (m, 3, Ph[3,4,5]); 8.49 (m, 2, Ph[2,6]). ^{13}C NMR (50 MHz, CD$_3$COCD$_3$, δ): 40.56 (NMe); 49.96, 54.26 (NMe$_2$); 57.19, 66.63 (CH$_2$); 129.75 (Ph[3,5]); 130.60 (Ph[2,6]); 133.21 (Ph[4]); 135.85 (Ph[1]); 236.13 (CO). IR (KBr): 1637 cm^{-1}. Anal. Calcd for C$_{17}$H$_{28}$N$_3$F$_3$O$_4$PdS: C, 38.24; H, 5.29; N, 7.87. Found: C, 38.21; H, 5.34; N, 7.92.

(4-Methoxybenzoyl){N,N,N′,N″,N″-pentamethyldi-ethylenetriamine}palladium Trifluoromethanesulfonate (6c). Yield: 79%. Mp: 144–147 °C (decomp). ^{1}H NMR (300 MHz, CD$_3$COCD$_3$, δ): 2.38 (s, 6, NMe$_2$); 2.75 (m, ABXY, 2, CH$_2$-CH$_2$-eq); 2.83 (m, ABXY, 2, CH$_2$CH$_2$-eq); 2.90 (s, 6, NMe$_2$); 2.92 (s, 3, NMe); 3.56 (m, ABXY, 2, CH$_2$CH$_2$-ax); 3.57 (m, ABXY, 2, CH$_2$CH$_2$-ax); 3.90 (s, 3, OMe); 7.07 (m, 2, Ph[3,5]); 8.47 (m, 2, Ph[2,6]). ^{13}C NMR (50 MHz, CD$_3$COCD$_3$, δ): 40.45 (NMe); 19.90, 54.22 (CH$_2$); 55.97 (OMe); 57.20, 66.57 (NMe$_2$); 114.78 (Ph[3,5]); 128.75 (Ph[4]); 132.73 (br, Ph[2,6]); 163.90 (Ph[1]); 233.10 (CO). IR (KBr): 1628 cm^{-1}. Anal. Calcd for C$_{18}$H$_{30}$N$_3$F$_3$O$_5$PdS: C, 38.34; H, 5.36; N, 7.45. Found: C, 38.29; H, 5.30; N, 7.50.

Reaction of Methyl{2,6-bis[(dimethylamino)methyl]-pyridine}palladium(II) Trifluoromethanesulfonate (1a) with Carbon Monoxide. Carbon monoxide (1 atm) was bubbled through an ice-cold solution of 232 mg of **1a** and 30 μL of 2,2-diphenylpropane (internal standard) in 2 mL CD$_3$-COCD$_3$ for 1 min, resulting in the immediate precipitation of palladium black. The reaction vessel was then closed, and the solution was stirred for 30 min at 0 °C. The solution was filtered through Celite and subsequently analyzed by GLC, GC–MS, and ^{1}H NMR spectroscopy. The conversion of **1a** was 100% as shown by ^{1}H NMR, and GLC analysis (SE-30 column) showed that acetic anhydride was formed in 84% yield (based on **1a**). GC–MS analysis of the NMR solution showed the sole formation of acetic anhydride ([M + H]$^+$ at m/e 103) which was confirmed by comparison with reference MS spectra. The ^{1}H NMR spectrum showed signals that correspond to acetic anhydride (2.20 ppm) and the quaternary ammonium salt [NN′(NH)]OTf (δ(NHMe$_2$) 4.85 ppm), respectively. The assignment of the acetic anhydride resonance was substantiated by addition of a tiny amount of acetic anhydride (15 μL). This resulted in the signal enhancement of the acetic anhydride methyl resonance, and no shifts or additional signals were observed. No resonances corresponding to acetylacetone, acetaldehyde, acetic acid, or diketene were observed.

High-Pressure NMR Studies of the Carbon Monoxide Insertion. A solution of 40 mg of the complex in 2 mL of CD$_3$-COCD$_3$ was transferred to a high-pressure NMR tube. The tube was then pressurized to 10 atm of carbon monoxide, and

Table 9. Coupling Constants[a] and Conformational Data of the NCH₂CH₂N Fragments in 5b–d and 6c,d[b]

R	$^2J_{a,b}$	$^2J_{a,c}$	$^2J_{a,d}$	$^2J_{b,c}$	$^2J_{b,d}$	$^2J_{c,d}$
MeCO 5b	−13.81 ± 0.18	3.17 ± 0.18	1.45 ± 0.13	13.30 ± 0.13	3.11 ± 0.17	−13.72 ± 0.17
Bz[c] 5c	−13.90 ● 0.27	3.41 ± 0.27	1.33 ± 0.27	13.29 ± 0.24	3.17 ± 0.35	−14.01 ± 0.32
4-MeOBz[c] 5d	−13.63 ± 0.72	3.33 ± 0.72	1.35 ± 0.72	13.17 ± 0.72	3.34 ± 0.72	−13.82 ± 0.72
Bz[c] 6c	−13.42 ± 0.65	3.09 ± 0.66	0.97 ± 0.11	13.87 ± 0.09	3.09 ± 0.63	−13.79 ± 0.64
4-MeOBz[c] 6d	−13.38 ± 0.86	3.11 ± 0.88	1.13 ± 0.13	13.89 ± 0.14	3.14 ± 0.91	−13.85 ± 0.93

R	X	Y	ω (deg)	n_δ
MeCO 5b	0.46 ± 0.05	4.20 ± 0.24	56.7 ± 0.7	1.06 ± 0.02
Bz[c] 5c	0.39 ± 0.08	3.90 ± 0.32	55.4 ± 1.0	1.06 ± 0.03
4-MeOBz[c] 5d	0.41 ± 0.23	3.95 ± 0.88	55.3 ± 3.0	1.07 ± 0.05
Bz[c] 6c	0.31 ± 0.08	4.49 ± 0.96	56.8 ± 2.7	1.11 ± 0.06
4-MeOBz[c] 6d	0.36 ± 0.11	4.47 ± 1.26	56.7 ± 3.6	1.10 ± 0.07

[a] In Hz, values and deviations were determined by spin simulation. [b] The assignments of the protons are shown in Figure 2. [c] Bz = benzoyl.

after 1.5 min inverted 5 times before transferring it to the NMR probe. The data collection for the first spectrum was started 2.5 min after pressurizing the tube. After 30 min the tube was again inverted 5 times. Spectra were obtained at regular intervals until either the conversion stopped above 50% before 30 min had passed or until 60 min had passed.

Conformational Analysis. NMR simulation of the experimental data gave accurate chemcial shifts and coupling constants with their standard deviations, allowing the determination of the conformation (δ or λ) and the NCCN torsion angle (ω) of the five-membered chelate rings using the following equations:[16]

$$n_\lambda = [X\cos^2\omega - \cos^2(120 - \omega)]/[\alpha\cos^2(120 + \omega) - \cos^2(120 - \omega)] \quad (3)$$

$$n_\lambda = [Y\cos^2\omega - \alpha\cos^2(120 + \omega)]/[\cos^2(120 - \omega) - \alpha\cos^2(120 + \omega)] \quad (4)$$

$$n_\lambda + n_\delta = 1 \quad (5)$$

where n_λ (n_δ) = the mole fraction of the λ (δ) conformation (Figure 2), $X = {}^3J_{a,d}/{}^3J_{a,c}$, and $Y = {}^3J_{b,c}/{}^3J_{a,c}$. A value of 1.208 was previously determined for the ratio of the Karplus constants (α).[16b] The standard deviations in the coupling constants (Table 9) were obtained from the NMR simulation, while those of X, Y, n_δ, and ω were obtained from these *via* standard mathematical methods.

Computational Details. The SCF calculations were carried out partly with the ASTERIX system of programs[30] and partly with the GAUSSIAN 92 system of programs[31] using the following basis set for the SCF geometry optimization: (15,9,8) contracted to ⟨6,4,4⟩ for the palladium atom;[32] (9,5) contracted to ⟨3,2⟩ for the first-row atoms;[34] and (4) contracted to ⟨2⟩ for the hydrogen atom.[35] The same basis set was used for the CAS−SCF and SD−CI+Q and the MP2 calculations.

Table 10. Crystal Data and Details of the Structure Determination of 4e

Crystal data	
empirical formula	C₂₃H₂₆F₃N₃O₄PdS
fw	603.95
cryst syst	triclinic
space group	P1̄ (No. 2)
a, b, c (Å)	8.742(1), 12.303(1), 13.563(1)
α, β, γ (deg)	116.33(1), 89.92(1), 103.47(1)
V_calcd (Å³)	1262.7(2)
Z	2
D_calcd (g/cm³)	1.588
F(000) (electrons)	612
μ(Mo Kα) (cm⁻¹)	8.6
cryst size (mm³)	0.05 × 0.10 × 0.50
Data Collection	
temp (K)	295
radiation, Mo Kα (Zr-filtered) (Å)	0.71073
θ_{min}, θ_{max} (deg)	0.1, 27.5
scan type	ω/2θ
scan (deg)	0.65 + 0.35 tan θ
ref refln(s)	1,−2,0; 1,0,−3; 0,4,−2
data set	0−11; −15 to 15; −17 to 17
tot., unique data	6775, 5784
no. of obsd data (I > 2.5σ(I))	4201
Refinement	
N_{ref}, N_{par}	330, 4201
R, wR, S	0.055, 0.052, 1.40
wting scheme, w^{-1}	$\sigma^2(F)$
max and av shift/error	0.16, 0.01
min and max resd density (e/Å³)	−0.80, 1.01

For the CAS−SCF calculations[36] on [Pd(NH₃)₂(CH₃)(CO)]⁺, [Pd(NH₃)₂(COCH₃)]⁺, and on the system with a geometry close to the transition state connecting them, the active space was made of 10 active orbitals populated by 12 electrons (10a12e CAS−SCF). This active space was set to account for the main bonding interactions and to remain coherent along the reaction path as much as possible. For the [Pd(NH₃)₂(CH₃)(CO)]⁺ reactant and for the structure close to the transition state of the insertion reaction the active orbitals turned out to be 4σ-(CO), 5σ(CO), π_z(CO), π_y(CO), 4d_{xz}(Pd), σ(CH₃) + 4$d_{x^2-y^2}$, 4$d_{x^2-y^2}$ − σ(CH₃), σ*(CO), π^*_z(CO), and π^*_y(CO), see Scheme 2 for the choice of axes. For the [Pd(NH₃)₂(COCH₃)]⁺ product, they turned out to be σ_{C-C}(COCH₃), σ_{C-O}(COCH₃), π_z(CO), π_y(CO), 4d_{xz}(Pd), [π^*_y(CO) + σ(CH₃)] + 4$d_{x^2-y^2}$, 4$d_{x^2-y^2}$ − [π^*_y(CO) + σ-(CH₃)], π^*_z(CO), σ*_{C-O}(COCH₃), and σ*_{C-C}(COCH₃) (with some 4p_x(O) character). For the CAS−SCF calculations on [Pd-(NH₃)₃(CH₃)]⁺ and [Pd(NH₃)₂(CH₃)···(NH₃)] + (Pd···NH₃ = 100 Å) the active space was made of eight active orbitals populated by eight electrons (8a8e CAS−SCF). The active orbitals were the three σ(NH₃), the σ(CH₃) orbitals and their correlated counterparts. The CI calculations were multireference con-

(30) (a) Ernenwein, R.; Rohmer, M.-M.; Bénard, M. *Comput. Phys. Commun.* **1990**, *58*, 305. (b) Rohmer, M.-M.; Demuynck, J.; Bénard, M.; Wiest, R. *Comput. Phys. Commun.* **1990**, *60*, 127. (e) Wiest, R.; Demuynck, J.; Bénard, M.; Rohmer, M.-M.; Ernenwein, R. *Comput. Phys. Commun.* **1991**, *62*, 107.

(31) Frisch, M. J.; Trucks, G. W.; Head-Gordon, M.; Gill, P. M. W.; Wong, M. W.; Foresman, J. B.; Johnson, B. G.; Schlegel, H. B.; Robb, M. A.; Reploge, E. S.; Gomperts, R.; Andres, J. L.; Raghavachari, K.; Binkley, J. S.; Gonzales, C.; Martin, R. L.; Fox, D. J.; Defrees, D. J.; Baker, J.; Stewart, J. J. P.; Pople, J. A. *Gaussian 92*, Revision, E.2.; Gaussian, Inc.: Pittsburgh, PA, 1992.

(32) The original (14,9,8) basis set[33] was modified by the addition of a p function of exponent 0.08386.

(33) Veillard, A. and Dedieu, A. *Theor. Chim. Acta* **1984**, *65*, 215.

(34) Huzinaga, S. *Technical Report*; University of Alberta: Edmonton, Canada, 1971.

(35) Huzinaga, S. *J. Chem. Phys.* **1965**, *42*, 1293.

(36) (a) Roos, B. O.; Taylor, P. R.; Siegbahn, P. E. M. *Chem. Phys.* **1980**, *48*, 157. (b) Siegbahn, P. E. M.; Almlöf, J.; Heiberg, A.; Roos, B. O. *J. Chem. Phys.* **1981**, *74*, 2384. (c) Roos, B. O. *Int. J. Quantum Chem., Symp.* **1980**, *14*, 175.

Table 11. Final Coordinates (Å) and Equivalent Isotropic Thermal Parameters (Å²) of the Non-Hydrogen Atoms for 4e

atom	x	y	z	$U_{eq}{}^a$
Pd	0.86503(5)	0.55189(4)	−0.15802(4)	0.0417(1)
O	0.7659(6)	0.5273(4)	0.0260(3)	0.086(2)
N(1)	0.9582(5)	0.4856(4)	−0.3051(3)	0.0480(17)
N(2)	0.6678(5)	0.4032(4)	−0.2581(4)	0.0545(17)
N(3)	1.0901(5)	0.6823(4)	−0.1139(4)	0.0515(17)
C(2)	0.8610(8)	0.3992(5)	−0.3944(5)	0.056(2)
C(3)	0.9228(9)	0.3437(6)	−0.4942(5)	0.069(3)
C(4)	1.0830(10)	0.3826(7)	−0.4957(6)	0.076(3)
C(5)	1.1814(8)	0.4732(6)	−0.4003(6)	0.067(3)
C(6)	1.1135(7)	0.5237(5)	−0.3035(5)	0.052(2)
C(7)	0.6896(7)	0.3794(6)	−0.3752(5)	0.064(2)
C(8)	0.6710(8)	0.2897(6)	−0.2465(6)	0.076(3)
C(9)	0.5114(7)	0.4309(7)	−0.2347(6)	0.078(3)
C(10)	1.1979(6)	0.6135(5)	−0.1888(5)	0.055(2)
C(11)	1.0730(8)	0.7843(6)	−0.1408(6)	0.072(3)
C(12)	1.1629(8)	0.7389(6)	0.0023(5)	0.068(2)
C(13)	0.7873(7)	0.6006(6)	−0.0122(5)	0.055(2)
C(14)	0.7539(7)	0.7273(5)	0.0510(5)	0.053(2)
C(15)	0.6873(7)	0.7722(6)	−0.0092(5)	0.063(2)
C(16)	0.6342(8)	0.8809(6)	0.0439(6)	0.075(3)
C(17)	0.6496(8)	0.9429(6)	0.1552(7)	0.076(3)
C(18)	0.7217(8)	0.9030(6)	0.2203(6)	0.065(3)
C(19)	0.7405(10)	0.9695(7)	0.3383(7)	0.096(3)
C(20)	0.8142(12)	0.9308(9)	0.3994(7)	0.113(4)
C(21)	0.8756(10)	0.8262(8)	0.3476(7)	0.099(4)
C(22)	0.8580(8)	0.7589(6)	0.2364(6)	0.071(3)
C(23)	0.7782(7)	0.7936(5)	0.1682(5)	0.057(2)
S	0.4087(3)	0.2353(2)	0.3197(2)	0.0879(9)
F(1)	0.3011(7)	0.0035(5)	0.2823(6)	0.157(3)
F(2)	0.1412(8)	0.1061(6)	0.3299(8)	0.231(5)
F(3)	0.2162(14)	0.0479(6)	0.1734(7)	0.265(5)
O(1)	0.3350(8)	0.3149(5)	0.3032(5)	0.123(3)
O(2)	0.4322(16)	0.2667(10)	0.4271(9)	0.327(8)
O(3)	0.5206(11)	0.2037(7)	0.2585(12)	0.306(8)
C(1)	0.2508(16)	0.0961(8)	0.2795(8)	0.122(5)

^{a} U_{eq} = $^1/_3$ of the trace of the orthogonalized **U** tensor.

tracted CI calculations[37] using as references the configurations which were found to have an expansion coefficient greater than 0.05 in the CAS−SCF wavefunction. A total of 12 electrons were correlated (the same as in the CAS−SCF wavefunction), and single and double excitations to all virtual valence orbitals were included. The CI results reported here include the Davidson correction[38] to provide an estimate of the inclusion of higher than double excitations.

The geometry optimization was carried out from analytical SCF energy first derivatives. In a few instances some internal coordinates were kept constant, *e.g.*, as to force C_s symmetry in the transition state determination of the insertion step. The final energies (au) with the methods in brackets, calculated for structures **I**−**XIII** were as follows **I**, −5135.1276 (SCF), −5135.7128 (MP2), −5135.2042 (CAS−SCF), −5135.2156 (SD−CI+Q); **II**, −5078.9403 (SCF); **II** + NH$_3$ (**II**···NH$_3$ = 100 Å), −5135.078 (SCF), −5135.6455 (MP2), −5135.1564 (CAS−SCF), −5135.1648 (SD−CI+Q); **III**, −5191.5662 (SCF),

−5192.2593 (MP2), −5191.7504 (CAS−SCF), −5191.8070 (SD−CI+Q); **IV**, −5191.5230 (SCF), −5192.2294 (MP2); **V**, −5191.5636 (SCF), −5192.2502 (MP2), −5191.7405 (CAS−SCF), −5191.8092 (SD−CI+Q); **VI**, −5247.7460 (SCF), −5248.5399 (MP2); **VII**, −5247.7253 (SCF), −5248.5233; **VIII**, −5247.7107 (SCF), −5248.5116 (MP2); **IX**, −5247.7138 (SCF), −5248.5216 (MP2); **X**, −5247.7074 (SCF); **XI**, −5247.7127 (SCF); **XIII**, −5247.6734 (SCF), −5248.4956 (MP2). The energy of NH$_3$ is as follows: −56.1316 (SCF), −56.2438 (MP2). The energy of CO is as follows: −112.5927 (SCF), −112.8015 (MP2).

X-ray Structure Determination of [Pd(1-naphthoyl)-(NN′N)]OTf (4e). A data set was collected for a needle-shaped crystal mounted on top of a glass fiber on an Enraf-Nonius CAD-4 diffractometer. Unit cell parameters were derived from the SET4 setting angles of 25 reflections in the range 9 < θ < 16°. The data were corrected for Lp, a small linear decay of 2.5%, and absorption (DIFABS;[39] correction range 0.78, 1.10). The structure was solved by Patterson techniques (SHELXS86/PATT[40]) and refined on F by full-matrix least-squares techniques (SHELX76[41]). Hydrogen atoms were taken into account at calculated positions (C−H = 0.98 Å) riding on their carrier atoms with two common isotropic thermal parameters. Some residual density in the triflate region (~1 e/Å³) indicates some disorder in that region. Scattering factors were taken from Cromer and Mann,[42] corrected for anomalous dispersion.[43] Geometrical calculations, including the ORTEP illustration, were done with PLATON.[44] Calculations were performed on a MicroVax-II cluster. Numerical details of the structure determination are given in Table 10, and positional data are collected in Table 11.

Supporting Information Available: Further details of the structure determination, including atomic coordinates, bond distances and angles, and thermal parameters (10 pages). Ordering information is given on any current masthead page.

OM950163+

(37) Siegbahn, P. E. M. *Int. J. Quantum Chem.* **1983**, *23*, 1869.
(38) Davidson, E. R. *The World of Quantum Chemistry*; Daudel, R., Pullman, B., Eds.; Reidel: Dordrecht, 1974.

(39) Walker, N.; Stuart, D. *Acta Crystallogr.* **1983**, *A39*, 158.
(40) Sheldrick, G. M. *SHELXS86, Program for Crystal Structure Determination*; University of Göttingen: Göttingen, Germany, 1986.
(41) Sheldrick, G. M. *SHELX76, Program for Crystal Structure Analysis Package*; University of Cambridge: Cambridge, U.K., 1976.
(42) Cromer, D. T.; Mann, J. B. *Acta Crystallogr.* **1968**, *A24*, 321.
(43) Cromer, D. T.; Liberman, D. *J. Chem. Phys.* **1970**, *53*, 1981.
(44) Spek, A. L. *Acta Crystallogr.* **1990**, *A46*, C34.